A canonical chloroplast unfolded protein response triggered by misfolded polypeptides

Alejo Cantoia[1,3], Fabricio Bertero[1], Rodrigo Berrocal[1], Eduardo A. Ceccarelli[1,3], Nicolás E. Blanco[2,*] and Germán L. Rosano[1,3,*]

[1]Instituto de Biología Molecular y Celular de Rosario (IBR), CONICET. Facultad de Ciencias Bioquímicas y Farmacéuticas, Universidad Nacional de Rosario. Rosario (2000), Argentina.

[2]Centro de Estudios Fotosintéticos y Bioquímicos (CEFOBI), CONICET. Facultad de Ciencias Bioquímicas y Farmacéuticas, Universidad Nacional de Rosario. Rosario (2000), Argentina.

[3]Unidad de Espectrometría de Masa (UEM-IBR), IBR, Rosario (2000), Argentina.

*Corresponding authors: rosano@ibr-conicet.gov.ar / blanco@cefobi-conicet.gov.ar

Keywords: unfolded protein response, chloroplast, CLPB3, disaggregase, protein quality control

ABSTRACT

Photosynthetic efficiency and plant viability rely on chloroplast protein homeostasis. While unfolded protein responses (UPRs) in the endoplasmic reticulum and mitochondria have been extensively characterized, the chloroplast UPR (cpUPR) remains less defined, partly due to the off-target effects of traditional stress-inducing methods. In this study, we provide direct evidence for the existence of the cpUPR by expressing engineered, folding-defective variants of ferredoxin-NADP$^+$ reductase (FNR) in plant chloroplasts. The expression of aggregation-prone proteins inside the organelle triggered a robust upregulation of chloroplast quality control components, including CLPB3, CLPC1/C2, and HSP90C, as revealed by immunodetection and quantitative proteomics. The proteomic response scaled with the severity of the folding defect, with the fully insoluble FNR Δ20 variant inducing broader changes than the partially soluble Δ3

variant. Network analysis showed that most differentially abundant proteins were chloroplastic and clustered into functional groups related to proteostasis and photosynthesis. Comparative analysis with lincomycin-treated plants highlighted the specificity and advantages of using misfolded proteins to study the cpUPR. Expression of the folding variants conferred tolerance to heat treatment, suggesting that the response can enhance plant fitness. Taken together, our work establishes the cpUPR as a specific stress response in chloroplasts and provides new tools for its characterization.

INTRODUCTION

Protein homeostasis, or proteostasis, refers to the balance between protein synthesis, folding, and degradation. Reaching a proper three-dimensional conformation is essential for protein solubility and function, and misfolding and aggregation can severely disrupt cellular physiology. Proteostasis is challenged by intrinsic factors such as errors in gene expression and by external stresses. Among these, abiotic stresses like elevated or freezing temperatures are particularly damaging, as they can destabilize protein structures, leading to misfolding, loss of function, and aggregation (Mogk et al., 2018). Cells can cope with the unfolded protein challenge by activating molecular responses that counterbalance the pathologic state. These pathways constitute the "unfolded protein response" (UPR), which comprises the activation of sensors and stress regulators that orchestrate an increase in the synthesis of proteins involved in quality control mechanisms, such as molecular chaperones and proteases (Hetz, 2012; Read & Schröder, 2021). The UPR is typically compartmentalized, and its molecular intricacies depend on the specific organelle affected. It was first discovered in the endoplasmic reticulum (Kozutsumi et al., 1988), where it is activated by the accumulation of misfolded proteins in the lumen under stress (erUPR). Similar responses were later found in the cytosol (Metzger & Michaelis, 2009; Wu, Meyer, Richter, et al., 2019) and other organelles, such as mitochondria (mtUPR) (Hoogenraad, 2017).

By its very definition, the UPR is triggered by the buildup of unfolded proteins within a cellular compartment. This state can be achieved in several ways. For instance, chemicals that interfere directly or indirectly with protein folding lead to the accumulation of unfolded or misfolded proteins. As an example, tunicamycin inhibits the initial stage of N-linked glycan production in the endoplasmic reticulum of eukaryotic cells, resulting in numerous misfolded proteins (Heifetz et al., 1979). In contrast, reducing agents like dithiothreitol impair oxidative protein folding (Braakman et al., 1992; Gopakumar & Singh, 2022). Cell treatment with these agents unleashes the erUPR (reviewed in Chapman et al., 1998). In mitochondria, treatments with paraquat (an inhibitor of the mitochondrial complex I that increases levels of reactive oxygen species) or CDDO (an inhibitor of the mitochondrial Lon1 protease) induce a potent mitochondrial unfolded protein response (mtUPR) (Münch & Harper, 2016; Shpilka & Haynes, 2018; Yoneda et al., 2004). These chemicals target critical enzymes involved in protein folding and degradation. For this reason, knockout organisms in the respective genes have also been extensively used to cause the accumulation of misfolded proteins (Shpilka & Haynes, 2018). On a larger scale, organismal-level abiotic stresses (e.g., heat shock) can also disrupt protein structure, generating responses with similar characteristics of a prototypical UPR.

Nevertheless, cell treatment with protein-folding disruptive chemicals or the use of knockout (or knockdown) organisms can activate other overlapping mechanisms, thereby obscuring the actual molecular signature of the UPR. A significant body of work suggests that pleiotropic effects in the chemically induced erUPR are numerous and activate additional counteractions beyond the prototypical UPR (Bergmann et al., 2018; Bergmann & Molinari, 2018; Gopakumar & Singh, 2022). Considering these issues, the sole accumulation of misfolded proteins appears as an unbiased strategy to trigger a true UPR. This approach has been used to differentiate the mtUPR and the erUPR from other mechanisms. In the former case, Zhao et al. used a folding-defective version of the mitochondrial protein ornithine transcarbamylase lacking residues 30 to 114 (Q. Zhao et al., 2002). Its expression in mitochondria resulted in the upregulation of

nuclear genes encoding chaperonin 60, chaperonin 10, mtDNAJ, and the protease CLPP, among others, leading to a significant increase in the levels of these proteins. The abundances of non-mitochondrial chaperones belonging to the erUPR (BiP, Grp94, protein disulfide isomerase, calnexin, and calreticulin) were not affected, indicating that accumulation of the folding-defective protein in mitochondria caused selective stress in the organelle (Q. Zhao et al., 2002). Using a similar approach, Hidvegi et al. employed HeLa cells that accumulated nonpolymerogenic versions of the ER-resident protein α1-antitrypsin, which lacked 19 residues from their C-terminus. An increase in the synthesis of the ER chaperone BiP was readily detected, a hallmark in the activation of the erUPR (Hidvegi et al., 2005).

In chloroplasts, a UPR (cpUPR) has been inferred from the use of chemicals, gene knockdowns, or systemic stresses that interfere with protein folding or degradation within the organelle. The cpUPR was first described in *Chlamydomonas reindhartii*, where an inducible system was devised to achieve reduced levels of the essential chloroplastic protease CLPP (Ramundo & Rochaix, 2014b). The damage is so extensive that this system ultimately leads to organelle autophagy. Later, it was found that lincomycin (LIN) treatment of *Arabidopsis thaliana* plantlets triggered a response with similar characteristics of a UPR (Llamas et al., 2017). LIN is an antibiotic that inhibits chloroplast translation by binding to plastid ribosomes. As ribosomes halt, nascent polypeptides cannot properly fold and aggregate. However, LIN also negatively affects the transcription rate of photosynthesis-related genes and decreases the phosphorylation level of the light-harvesting complex II (Mulo et al., 2003). Moreover, it can affect chloroplast biogenesis and development, as well as the expression of light- and hormone-responsive genes and the circadian rhythm (Ruckle et al., 2012). Finally, systemic abiotic stresses also trigger cpUPR-like mechanisms. High-light treatment of leaves causes photooxidative damage to the photosystem II reaction center proteins, such as D1 and D2. The impaired proteins are targeted and degraded by the thylakoid-anchored metalloprotease FTSH2, also called VAR2 (Kato et al., 2012). Inactivation of FTSH2 in *var2* mutants grown under continuous light leads to the accumulation

of damaged proteins in chloroplasts. At the same time, it also results in the buildup of reactive oxygen species, which could then disturb the redox balance within the chloroplasts, magnifying the disruption of proteostasis. Both phenomena trigger a cpUPR-like response, termed cpUPR-like damaged protein response (DPR) (Dogra et al., 2019). Altogether, these pioneering works used chemicals, knockdown organisms, and abiotic stresses to unleash protective molecular responses in plastids. Alas, their off-target effects on other cellular compartments or molecular components activate overlapping or unspecific pathways, which cannot be distinguished from the actual cpUPR.

Our work introduces the novel application of folding-defective proteins as triggers for the chloroplast unfolded protein response. We used two variants of ferredoxin NADP+ reductase (FNR) engineered to display folding defects. FNR is a monomeric, highly soluble enzyme that contains noncovalently bound FAD as a prosthetic group. It catalyzes the electron transfer from ferredoxin, reduced by photosystem I, to NADP+. Its carboxyl-terminal region includes most of the NADP(H) binding residues, some of which also participate in the non-covalent binding of the FAD ligand. To evaluate the impact of the accumulation of folding variants in chloroplasts, we used two approaches: transient transformation of *Nicotiana benthamiana* leaves and stable transformation of *A. thaliana*. Through comprehensive proteomics analysis and other techniques, we sought to unravel the network of proteins involved in the cpUPR and uncover the differences between the responses triggered by LIN treatment.

MATERIALS AND METHODS

Plasmid construction

The construction of *Pisum sativum* FNR variants with reduced solubility was described in Orellano et al. The FNR Δ3 variant lacks Asp289, Trp290, and Ile291 residues. In contrast, the Δ20 deletion variant (FNR Δ20) lacks the last 20 residues from the C-terminal end. Coding sequences of wild-type FNR (FNR WT) and the aggregation-prone forms were cloned into the

plant expression vector pCHF3. The coding sequence of the transit peptide from *A. thaliana* FNR leaf isoform 1 from chloroplasts was added to each construct to direct the proteins into the organelle. For confocal microscopy imaging, the cyan fluorescence protein (CFP) coding sequence, which was codon optimized for plant expression, was inserted between the transit peptide and the FNR variants. All cloning procedures were performed using RF cloning, and plasmid construction was verified through DNA sequencing.

Plant transformation

The pCHF3 plasmids were introduced into the *Agrobacterium tumefaciens* strain GV3101-pMP90 by electroporation. For transient expression assays, the transformed *A. tumefaciens* cells harboring each vector were cultured until the late exponential phase, then centrifuged and resuspended in infiltration buffer (10 mM MES, pH 5.0, 10 mM $MgCl_2$, and 200 µM acetosyringone) to achieve an optical density of 0.7 at 600 nm. Subsequently, each culture was utilized for leaf infiltration in 4-week-old *N. benthamiana* plants (Blanco et al., 2019).

Following agroinfiltration, the plants were maintained under control conditions in a growth chamber with a 16-hour photoperiod at 23°C during the day and 18°C at night for varying post-infiltration (PI) durations as required by the experiment. To generate plants with stable expression of the FNR variants, inflorescences of *A. thaliana* (Col-0 ecotype) were subjected to agrotransformation using the floral dip method (Clough & Bent, 1998). Seeds obtained from the transformed plants were subjected to surface sterilization and subsequently placed on plates containing 0.5× Murashige-Skoog salts, 0.8% agar, and 50 µg/mL kanamycin for selection purposes.

Chloroplast isolation

4-week-old *N. benthamiana* plants were agroinfiltrated, as previously explained. 72 hours PI, they were transferred to darkness for 24 hours. To begin, the leaves were washed with cold

distilled water and then homogenized using a Polytron blender for 15 s in the presence of cold CIB buffer (50 mM HEPES, pH 7.5, 330 mM sorbitol, 2 mM EDTA, 1 mM $MgCl_2$, 0.25% w/v bovine serum albumin, 100 mM glutathione). The homogenized material was filtered through two layers of Miracloth, and the liquid was collected in a beaker. This homogenization and filtration step was repeated five times. The suspension was centrifuged for 15 min at 4000 rpm in a refrigerated centrifuge. After removing the supernatant, the chloroplasts were resuspended in 2 mL of CIB buffer using a paintbrush. The suspension was centrifuged on a Percoll (Percoll Plus, GE) discontinuous gradient (40%/80% layers in CIB buffer) at 7500 rpm for 30 min using a swinging bucket rotor to enrich the solution with intact chloroplasts, which migrate at the 40%/80% Percoll interphase. The chloroplasts were then transferred to a clean tube for washing with HF buffer (50 mM HEPES, pH 7.5, 330 mM sorbitol). Finally, a liquid nitrogen shock was applied to rupture the chloroplasts, and the samples were resuspended in denaturing sample buffer (1X) for SDS-PAGE electrophoresis.

High-temperature treatment of plants

28-day-old *A. thaliana* plants were subjected to heat stress treatment in controlled environmental chambers (Fitotron, 60% relative humidity). T0 generation transgenic lines expressing pea FNR WT or folding variants and a control line transformed with the empty vector (pCHF3) were grown under identical conditions and treated in parallel. The heat stress protocol consisted of a preconditioning step, during which plants were incubated for 12 h at 19°C in darkness, followed by a heat shock phase at 45°C for 12 h under constant illumination (100 µmol m^{-2} s^{-1}). In parallel, a non-stressed control group was incubated for the same 12-hour period under identical light and humidity conditions but at 22°C to assess normal growth.

Confocal microscopy

Laser confocal scanning microscopy was performed using a Plan Apochromat 20x, 0.8-NA lens on an LSM880 Zeiss microscope, with the 458-nm laser line for excitation. The fluorescence

emission was collected between 463 and 517 nm for CFP and 666 and 735 nm for chlorophyll. Cellular parameters and fluorescence intensities were analyzed with Fiji (Schindelin et al., 2012).

Western blot analysis

Homogenates were prepared from leaf tissue by pulverization in liquid nitrogen, followed by resuspension in lysis solution (100 mM Tris-HCl pH 8, 10 mM $MgCl_2$, 25 mM DTT, 1 mM EDTA, 20% v/v glycerol, and 1 mM phenylmethylsulfonyl fluoride). The extract was centrifuged at 12,000 g and 4°C for 15 minutes, and the resulting supernatant was used for protein separation by electrophoresis and immunodetection assays. Total protein content was quantified using the Bradford method. The protein extracts were separated by SDS-PAGE in 10% polyacrylamide gels and then transferred to nitrocellulose sheets. During the Western blot procedure, primary antibodies were used at a dilution of 1:3000, including anti-FNR (rabbit, AS15 2909, Agrisera), anti-CLPC (rabbit, AS01 001, Agrisera), and anti-CLPB3 (Parcerisa et al., 2020). Different types of secondary anti-rabbit IgG antibodies were used. In assays using enzyme-conjugated antibodies, alkaline phosphatase-conjugated antibodies were used at a dilution of 1/8000. In other immunodetection assays, chemiluminescence detection was employed using HRP-conjugated antibodies from Bio-Rad and the commercial detection kit provided by the same supplier (Inmun-Star HRP).

Sample preparation and LC-MS/MS analysis

Protein extracts prepared as described were subjected to SDS-PAGE, with electrophoresis carried out until the proteins had migrated approximately 1 cm into the resolving gel. The gel section was excised, and proteins were reduced with 10 mM dithiothreitol in 50 mM ammonium bicarbonate at 56 °C for 45 min, followed by alkylation with 55 mM iodoacetamide in 50 mM ammonium bicarbonate in the dark at room temperature for 30 min. Gel pieces were then washed, dehydrated with acetonitrile, and rehydrated with sequencing-grade trypsin (Promega) at a concentration of 12.5 ng/µL in 50 mM ammonium bicarbonate. Digestion was carried out

overnight at 37 °C. Peptides were extracted with 100% v/v acetonitrile, followed by 0.5% v/v trifluoroacetic acid, dried by vacuum centrifugation, and resuspended in 1% v/v formic acid.

Peptide separations were conducted using a nano HPLC Ultimate3000 system (Thermo Scientific) equipped with a nano column (EASY-Spray ES903, 50 cm × 50 µm ID, PepMap RSLC C18). The mobile phase consisted of 0.1% formic acid in water (solvent A) and 0.1% formic acid in acetonitrile (solvent B) at a 300 nL/min flow rate. The gradient profile was programmed as follows: (i) for LIN treatment: 4 – 30% solvent B over 114 min, 30 – 80% solvent B over 14 min, and 80% solvent B for 2 min; (ii) for proteomic comparison of plants expressing FNR variants: 4 – 35% solvent B over 90 min, 35 – 90% solvent B over 20 min, and 90% solvent B for 5 min. Mass spectrometry analysis was performed using a Q-Exactive HF mass spectrometer (Thermo Scientific). Ionization was achieved with a liquid junction voltage of 1.9 kV and a capillary temperature of 250°C. The full scan method employed a mass range of m/z 375–1,600, with an Orbitrap resolution of 120,000 (at m/z 200). The automatic gain control (AGC) target was set to 2×10^5, and the maximum injection time was 32 ms. After the survey scan, the 20 most intense precursor ions were selected for MS/MS fragmentation. Fragmentation was performed with a normalized collision energy of 27 eV, and MS/MS scans were acquired with a dynamic first mass. The AGC target for MS/MS was also 2×10^5, with a resolution of 15,000 (at m/z 200). An intensity threshold of 2.5×10^5 was applied, and an isolation window of 1.4 m/z units was used. The maximum injection time for MS/MS scans was 32 ms. To improve data quality, charge state screening was enabled to reject unassigned, singly charged ions and ions with eight or more charges. A dynamic exclusion time of 30 s was implemented to prevent the re-selection of previously analyzed ions.

MS data analysis

MS data were analyzed using standardized workflows with Proteome Discoverer (V: 2.4.1.15). Mass spectra *.raw files were searched against the reviewed protein database from *A. thaliana*

(Mouse-ear cress, cv Columbia), entry UP000006548 from UniProt. Precursor and fragment mass tolerances were set to 10 ppm and 0.02 Da, respectively, allowing for up to two missed cleavages. Fixed modification: carbamidomethylation of cysteines. Dynamic modifications: protein N-terminal acetylation and/or methionine loss and methionine oxidation. The mass spectrometry proteomics data have been deposited to the ProteomeXchange Consortium *via* the PRIDE partner repository with the dataset identifier PXD064779 (Perez-Riverol et al., 2025).

The normalized abundances were uploaded to the Perseus platform for quality control and statistical analysis (Tyanova et al., 2016). Network analysis was conducted in Cytoscape, utilizing the StringApp to retrieve protein-protein interaction information and Gene Ontology (GO) terms. Clustering was performed using the clusterMaker app, and the MCL algorithm was applied with default settings.

RESULTS

Expression of FNR Δ3 in chloroplasts increases the levels of the CLPB disaggregase

Our working hypothesis is that the accumulation of unfolded proteins in the chloroplast is sufficient to unleash the cpUPR. We chose ferredoxin-NADP+ reductase (FNR) from pea as a model. We have previously shown that deletions at the C-terminus are detrimental to catalysis and solubility. Eliminating the triad Asp289, Trp290, and Ile291 leads to a complete loss of catalytic activity and a 50% reduction in solubility compared to the wild-type enzyme (Orellano et al., 1993). The deletion mutant FNR Δ3 does not bind FAD, as evidenced by the lack of the characteristic yellowish color of recombinant FNR preparations from bacterial cells (Figure 1). A more extensive truncation, FNR Δ20, removes the final 20 amino acids, further reducing solubility and resulting in an entirely insoluble protein. This Δ20 variant will be used in subsequent experiments to assess the effects of expressing an unfolded protein in *A. thaliana*.

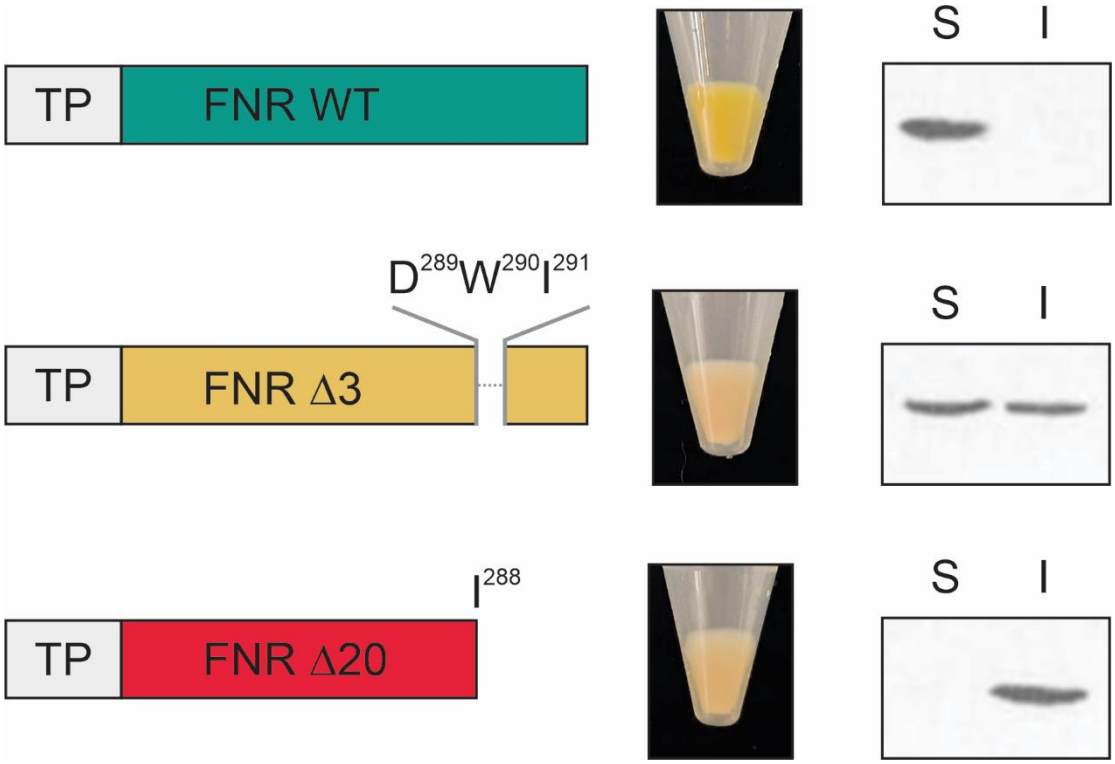

Figure 1: Expression and solubility of FNR C-terminal variants. Left: schematic representations of coding sequences for TP-FNR wild-type (WT), TP-FNR Δ3 (lacking residues D289–I291), and TP-FNR Δ20 (truncated at residue 288). Molecular mass of TP: 5.1 kDa. Middle: bacterial pellets show loss of FAD-dependent yellow color in both deletion variants. Right: Western blot of soluble (S) and insoluble (I) fractions, showing that solubility decreases with increasing C-terminal truncation.

The localization of the proteins to the chloroplast was achieved by fusing the transit peptide (TP) of *A. thaliana* FNR leaf isoform 1 from chloroplasts to the different pea FNR versions. This TP successfully directs proteins to the organelle in many plant species. Moreover, *in silico* analysis of the constructs by TargetP-2.0 indicated a high probability of chloroplast localization for all FNRs (Almagro Armenteros et al., 2019). TP-FNR WT and TP-FNR Δ3 coding sequences were cloned in the binary vector pCHF3 downstream of the 35S promoter for constitutive expression and used to transiently transform *N. benthamiana* leaves by agroinfiltration. Overexpression of

FNR WT was confirmed by Western blot analysis of total *N. benthamiana* leaf extracts, showing detectable accumulation 48 hours post-infiltration, which persisted for at least four days (Figure 2A). The anti-FNR antibodies crossreact with the endogenous *N. benthamiana* FNR and the heterologous pea FNR WT (molecular mass of the mature forms: 34.6 and 34.8 kDa, respectively), as indicated by the signal observed in plant extracts transformed with the empty vector. The strong signal observed in plants overexpressing FNR WT reflects the combined contribution of endogenous and exogenous FNR. However, overexpression of FNR Δ3 does not noticeably increase the intensity of the comigrating band despite differing from FNR WT by only three amino acids. When detection was performed on chloroplast-enriched fractions, faint expression of FNR Δ3 could be visualized as a band slightly more intense than in plants infiltrated with the empty vector (Figure 2B). Notably, no precursor forms of either protein were detected, suggesting that both FNR WT and FNR Δ3 were efficiently imported into chloroplasts and processed to their mature forms.

One known molecular signature of the response to LIN treatment is the increase in the abundance of the chloroplastic chaperone CLPB (Llamas & Pulido, 2022). We have previously demonstrated the disaggregase activity of CLPB3 from *A. thaliana* (Parcerisa et al., 2020). We, therefore, investigated its abundance in whole leaf extracts and isolated plastids from agroinfiltrated leaves expressing FNR WT and FNR Δ3. At 48 h post-infiltration, a marked increase in CLPB levels was observed in leaves expressing FNR Δ3. In contrast, CLPB levels in FNR WT-expressing leaves were comparable to those of controls. CLPB levels further increased at 90 h, indicating a sustained response (Figure 2A). In isolated plastids from FNR Δ3-expressing leaves, the accumulation of CLPB was even more pronounced compared to FNR WT and control samples (Figure 2B). These findings suggest that the misfolding-prone FNR Δ3 variant triggers a proteostatic stress response in chloroplasts, consistent with the activation of a cpUPR-like pathway.

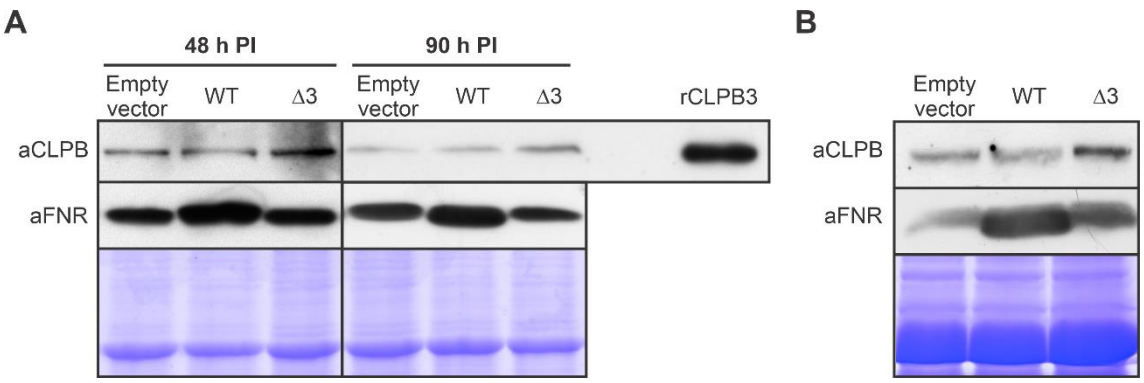

Figure 2. Differential expression and chloroplast stress response induced by FNR WT and Δ3 variants in *N. benthamiana*. (A) Total protein extracts from *N. benthamiana* leaves transiently transformed *via* agroinfiltration with the binary vector pCHF3, encoding plastid-targeted FNR WT or Δ3 under the control of the 35S promoter, were analyzed by immunoblotting at 48 and 90 hours post-infiltration (h PI). Detection was performed using antibodies against FNR (aFNR) and CLPB (aCLPB). Extracts from plants infiltrated with the empty vector served as controls. Coomassie-stained gels show equal protein loading. Recombinant *A. thaliana* CLPB3 (rCLPB3) was used as a positive control for antibody specificity. (B) Chloroplast-enriched fractions from the same samples (collected at 90 h PI) revealed a pronounced accumulation of CLPB in plastids from Δ3-expressing leaves.

Confirmation of the accumulation of FNR WT and, especially, FNR Δ3 in chloroplasts was obtained using confocal microscopy with variants fused to CFP. Signals were confined to chloroplasts, as judged by colocalization with chlorophyll autofluorescence (Figure 3). Consistent with Western blot analyses, the CFP-FNR WT signal exhibited greater intensity and a broader distribution than the CFP-FNR Δ3 signal. Altogether, the data indicate that our chloroplast-targeted expression system can be used to trigger a CLPB-mediated unfolded protein response.

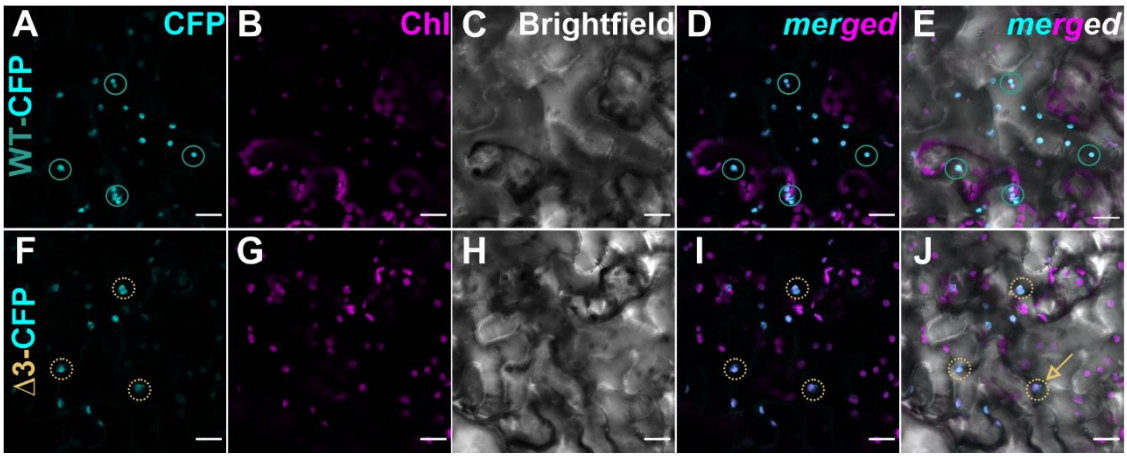

Figure 3: Subcellular localization of CFP-FNR WT and CFP-FNR Δ3 in *N. benthamiana* epidermal cells. FNR WT and FNR Δ3, fused to CFP and targeted to plastids using the *A. thaliana* FNR TP, were transiently expressed in *N. benthamiana* leaves. Confocal laser scanning microscopy images show CFP fluorescence (cyan; A, F), chlorophyll autofluorescence (magenta; B, G), and brightfield views (C, H). Merged images of fluorescence channels (D, I) and merged with brightfield (E, J) are shown. Green (WT, top panels) and orange (Δ3, bottom panels) circles highlight CFP signals overlapping with chlorophyll autofluorescence, indicating chloroplast localization. A yellow arrow in panel J marks the CFP-FNR Δ3 signal within stromules, dynamic extensions of chloroplasts. Scale bars: 20 µm.

***A. thaliana* plants expressing FNR deletion variants show a cpUPR**

Having established that the expression of a misfolded protein in chloroplasts leads to increased levels of the disaggregase CLPB in transient expression assays, we next aimed to investigate the molecular features of this response in greater detail. To this end, we expanded our experimental model in two ways. First, we adopted a stable expression system in *A. thaliana*, which provides flexibility to explore developmental conditions, robustness, and simplicity. Second, we introduced an additional FNR folding variant with enhanced aggregation propensity. Specifically, the deletion of the C-terminal 20 amino acids in FNR results in a pronounced loss of solubility;

this mutant, referred to as FNR Δ20, is unable to fold. Including this variant enabled us to probe how the degree of misfolding affects the chloroplast's proteostasis machinery.

We transformed flowering *A. thaliana* plants using the floral dip method with *A. tumefaciens* strains harboring the same plasmids used in transient expression assays. An additional strain carrying pCHF3 with the coding sequence for TP-FNR Δ20 was included. Plants from the T0 generation onward exhibited no noticeable phenotypic differences compared to controls. The expression of the pea FNR proteins in *A. thaliana* T0 plants was assessed using orthogonal techniques. First, the expression and chloroplast localization of FNR WT and the folding variants were confirmed by confocal microscopy using CFP fusions. Results mirrored those in *N. benthamiana*: FNR WT–CFP showed strong organellar localization, while the folding variants exhibited weaker and less frequent CFP signals (Figure 4).

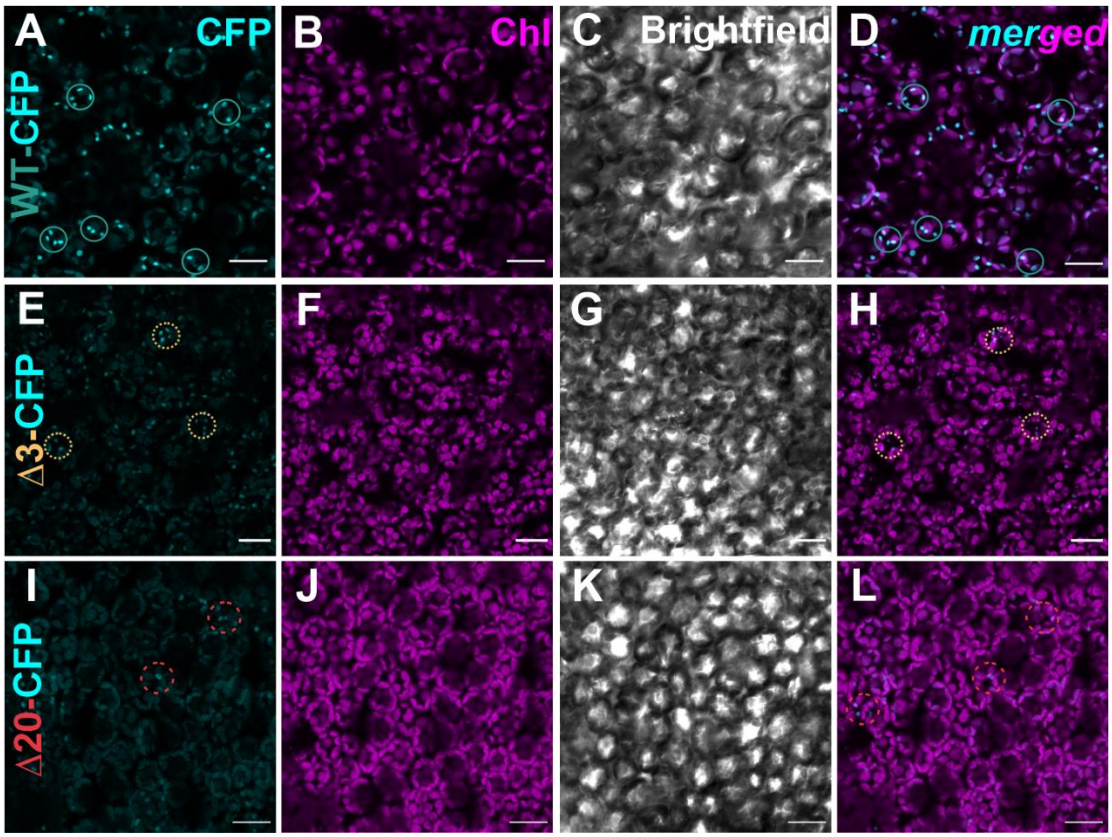

Figure 4. Subcellular localization of FNR WT, Δ3, and Δ20 variants fused to CFP in *Arabidopsis thaliana* transgenic plants. Confocal laser scanning microscopy images of leaf epidermal cells

from *A. thaliana* plants stably overexpressing CFP-FNR WT (A–D), CFP-FNR Δ3 (E–H), or CFP-FNR Δ20 (I–L). The CFP fluorescence signal (cyan) is shown in panels A, E, and I; chlorophyll autofluorescence (magenta) is shown in panels B, F, and J; and corresponding brightfield images in panels C, G, and K. Merged images (D, H, L) combine CFP and chlorophyll signals to assess colocalization. Colored circles highlight representative regions where CFP signal overlaps with chlorophyll autofluorescence, indicating plastid localization: green in A and D (FNR WT), orange in E and H (FNR Δ3), and red in I and L (FNR Δ20). Scale bars: 20 µm.

To obtain more evidence that the pea FNR variants were being expressed in transformed *A. thaliana* plants, we sought to detect unique peptides of the pea variants in leaf extracts by mass spectrometry. Unique peptides refer to tryptic peptides that are only found in the pea variants and are absent in the endogenous FNRs. For example, the tryptic peptides "MAQYAEELWELLKK" and "LVYTNDAGEVVK" are specific to FNR WT, FNR ∆3, and FNR ∆20. These peptides were indeed detected in leaf extracts from all plants expressing pea FNRs, indicating their successful expression (Figure 5A and B). Of note, the pea FNR-specific tryptic peptide "DGIDWIEYKR" (which includes the DWI triad removed in FNR ∆3 and from where the deletion in FNR ∆20 starts) could only be found in plants expressing pea FNR WT (Figure 5C). Consistently, the number of peptide spectrum matches of pea FNR peptides in plants expressing FNR WT was higher than in plants expressing the mutants. This again reflects its greater abundance in leaves. Finally, we could not detect any tryptic peptide from the TP, which suggests that preproteins were being readily processed into their mature form.

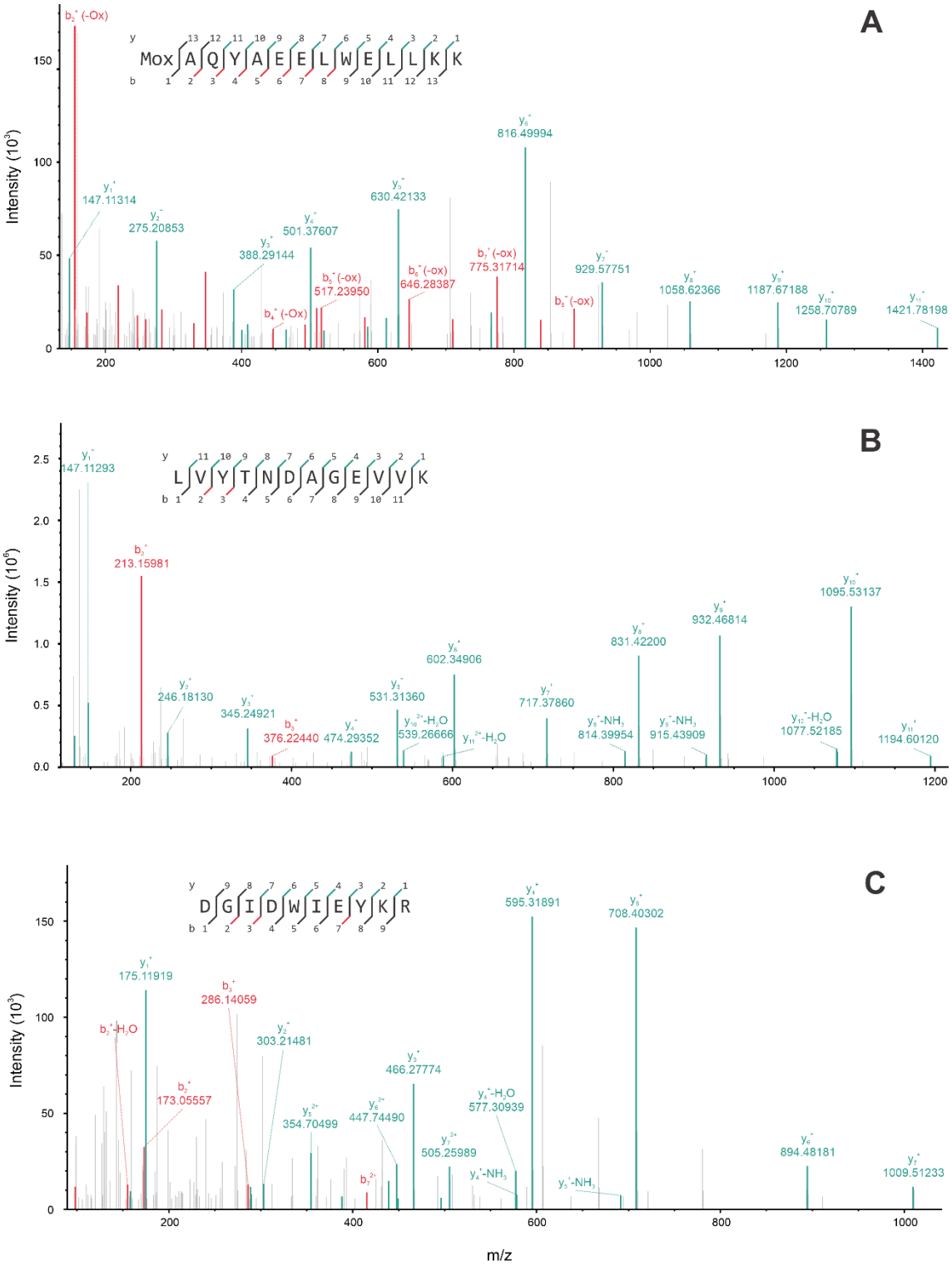

Figure 5. MS2 spectra of unique tryptic peptides from pea FNR variants expressed in *A. thaliana*. (A) Spectrum of the MAQYAEELWELLKK bearing and oxidized methionine residue (Mox), specific to all pea FNR variants (WT, Δ3, and Δ20). (B) Spectrum of the variant-specific peptide LVYTNDAGEVVK, also shared by FNR WT, Δ3, and Δ20. (C) Spectrum of the peptide

DGIDWIEYKR, found exclusively in plants expressing pea FNR WT, as it contains the DWI motif absent in FNR Δ3 and FNR Δ20. b- and y-ion series are indicated in red and blue-green, respectively.

Immunodetection of the FNRs in *A. thaliana* leaves yielded similar results to those of *N. benthamiana*. Again, the anti-FNR antibodies crossreact between the endogenous *A. thaliana* FNR isoforms (FNR1 and FNR2) and the alien pea FNR isoforms. An increased signal was detected only in plants overexpressing FNR WT (Figure 6A and B). A double band was visible in these plants, consistent with the molecular mass difference between *A. thaliana* FNRs in their mature forms (35.3 kDa) and pea FNR WT (34.8 kDa). The folding-defective variants FNR Δ3 and FNR Δ20 are not present in sufficient quantities to be detected by this technique. To explore the cpUPR in the *Arabidopsis* model, we checked the levels of candidate proteins involved in quality control by Western blot. The levels of CLPB3, the chloroplastic disaggregase from *A. thaliana*, as well as those of CLPC (CLPC1 and CLPC2) significantly increased by as much as six (CLPB3) and three (CLPC) times in plants expressing FNR Δ3 or FNR Δ20 compared to controls or plants expressing FNR WT (Figure 6A and B). As previously observed for CLPB in *N. benthamiana*, the expression of aggregation-prone FNR variants in *A. thaliana* chloroplasts leads to an increase in the levels of quality control proteins to sustain proteostasis.

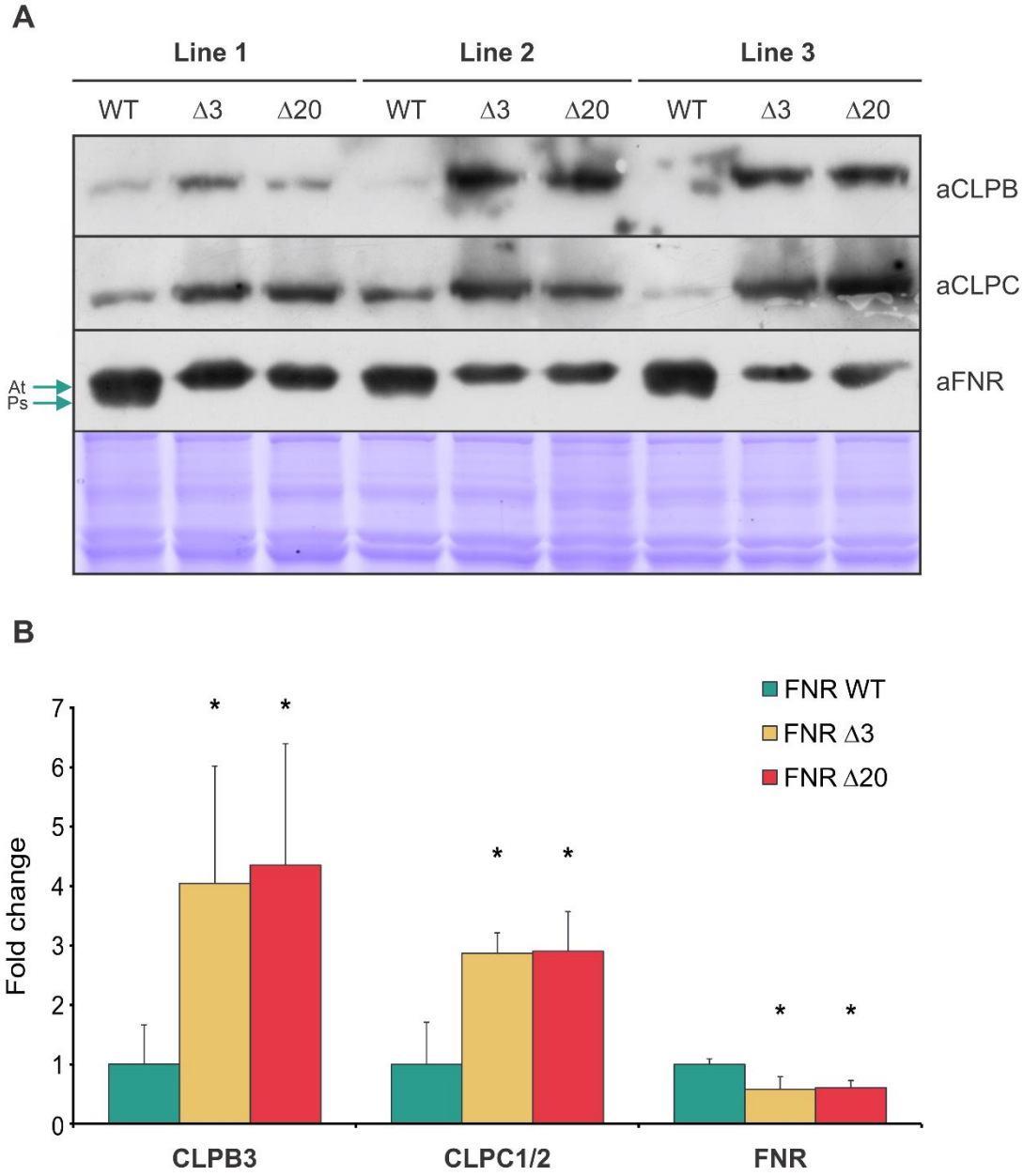

Figure 6: Immunodetection of FNR variants and chloroplast quality control proteins in *A. thaliana* plants expressing pea FNRs. (A) Immunoblots showing CLPB3, CLPC1/2, and FNR levels in three independent transgenic lines of *A. thaliana* expressing pea FNR WT, FNR Δ3, or FNR Δ20. Equal loading was confirmed by staining of total protein (bottom panel). The anti-FNR antibody (aFNR) detects endogenous *A. thaliana* isoforms (FNR1 and FNR2) and exogenous pea FNRs. A double band is observed in FNR WT-expressing plants, consistent with the size difference between endogenous and pea FNRs. aCLPB and aCLPC, antibodies against CLPB3 and CLPC,

respectively. (B) Quantification of protein levels from panel A. Bars represent mean fold change ± SD (n = 3). Asterisks denote statistically significant differences relative to FNR WT ($p < 0.05$).

The degree of misfolding shapes the cpUPR response

To gain further insight into the molecular response of plants coping with the expression of FNR variants, we analyzed the leaf proteome using high-resolution mass spectrometry. Protein extracts from four biological replicates of *A. thaliana* expressing pea FNR WT, Δ3, or Δ20 were subjected to tryptic digestion and analyzed via a label-free quantification strategy. Intragroup Pearson correlation coefficients were above 0.96, indicating excellent reproducibility and technical consistency (Figure 7A). Principal component analysis revealed a clear separation between samples expressing FNR WT and those expressing the folding-defective variants, suggesting a distinctive change in the proteome under these conditions (Figure 7B).

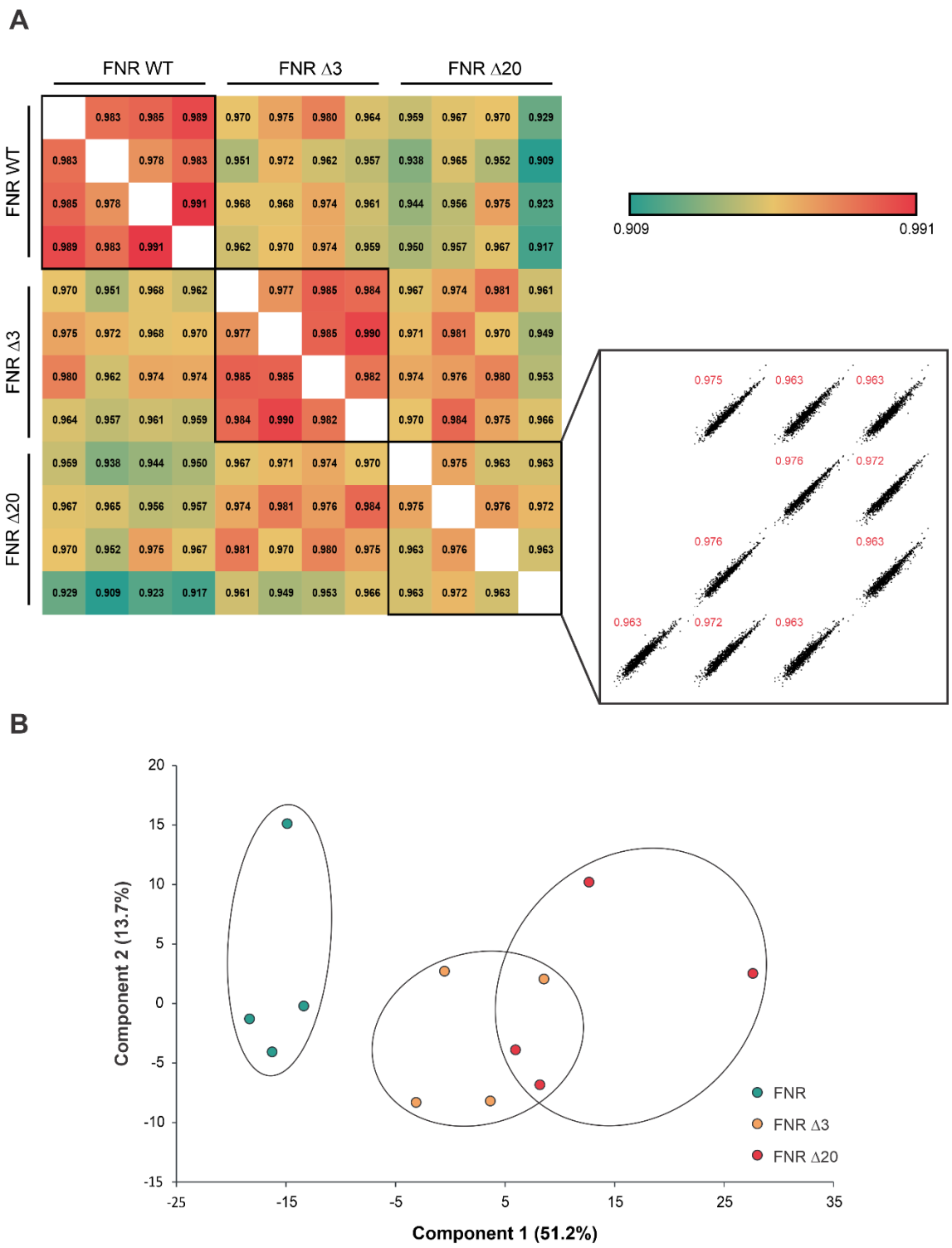

Figure 7: Proteomic analysis of *A. thaliana* plants expressing FNR variants. (A) Pearson correlation matrix of label-free quantitative proteomics data from *A. thaliana* expressing pea FNR WT, FNR Δ3, or FNR Δ20. Four biological replicates were analyzed per condition. Inset: scatter plots of selected replicate comparisons, with correlation values indicated in red.

(B) Principal component analysis of the proteomic profiles. Component 1 (51.2%) and 2 (13.7%) capture the major variance in the dataset. PCA reveals the separation of FNR WT samples from those expressing the folding-defective variants (FNR Δ3 and FNR Δ20), indicating distinct proteomic responses associated with the accumulation of misfolded FNR.

Next, we analyzed the differential abundance of proteins that were significantly regulated. The expression of FNR Δ3 resulted in an increased abundance of 156 proteins and a downregulation of 26, compared to FNR WT. At the same time, FNR Δ20 variant induced a broader shift, with 239 proteins upregulated and 17 downregulated, suggesting a more extensive response to this aggregation-prone variant (Supplementary Table 1). Figure 8A summarizes the number of differentially expressed proteins and illustrates the overlaps and specificities among the different comparisons. Notably, over 90% of the DEPs observed in Δ3-expressing plants were also present in the Δ20 background, indicating that the response to FNR Δ3 represents a subset of the more extensive alterations induced by Δ20. To visualize expression patterns, we generated a heatmap of all differentially expressed proteins across genotypes (Figure 8B). Hierarchical clustering separated the genotypes and identified two prominent protein groups. One cluster is upregulated only in Δ20, while the other shows upregulation from WT to Δ3 and Δ20. These trends suggest the activation of both shared and variant-specific pathways.

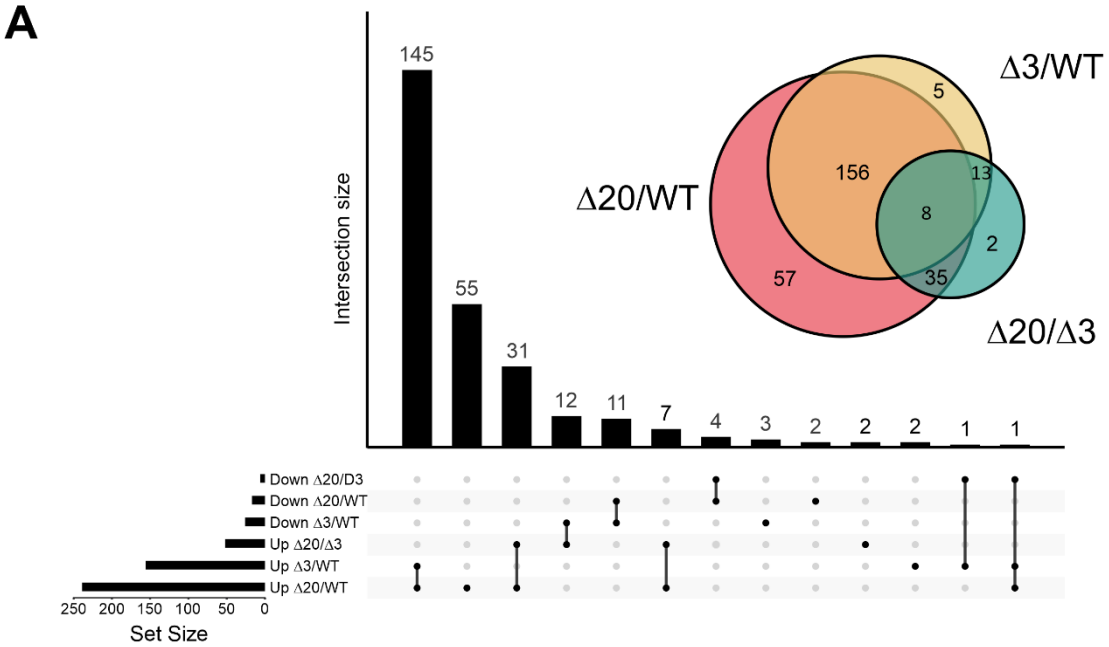
A
Intersection size
145
55
31
12
11
7
4
3
2
2
2
1
1
Δ3/WT
Δ20/WT
Δ20/Δ3
5
156
13
8
2
57
35
Down Δ20/D3
Down Δ20/WT
Down Δ3/WT
Up Δ20/Δ3
Up Δ3/WT
Up Δ20/WT
250 200 150 100 50 0
Set Size

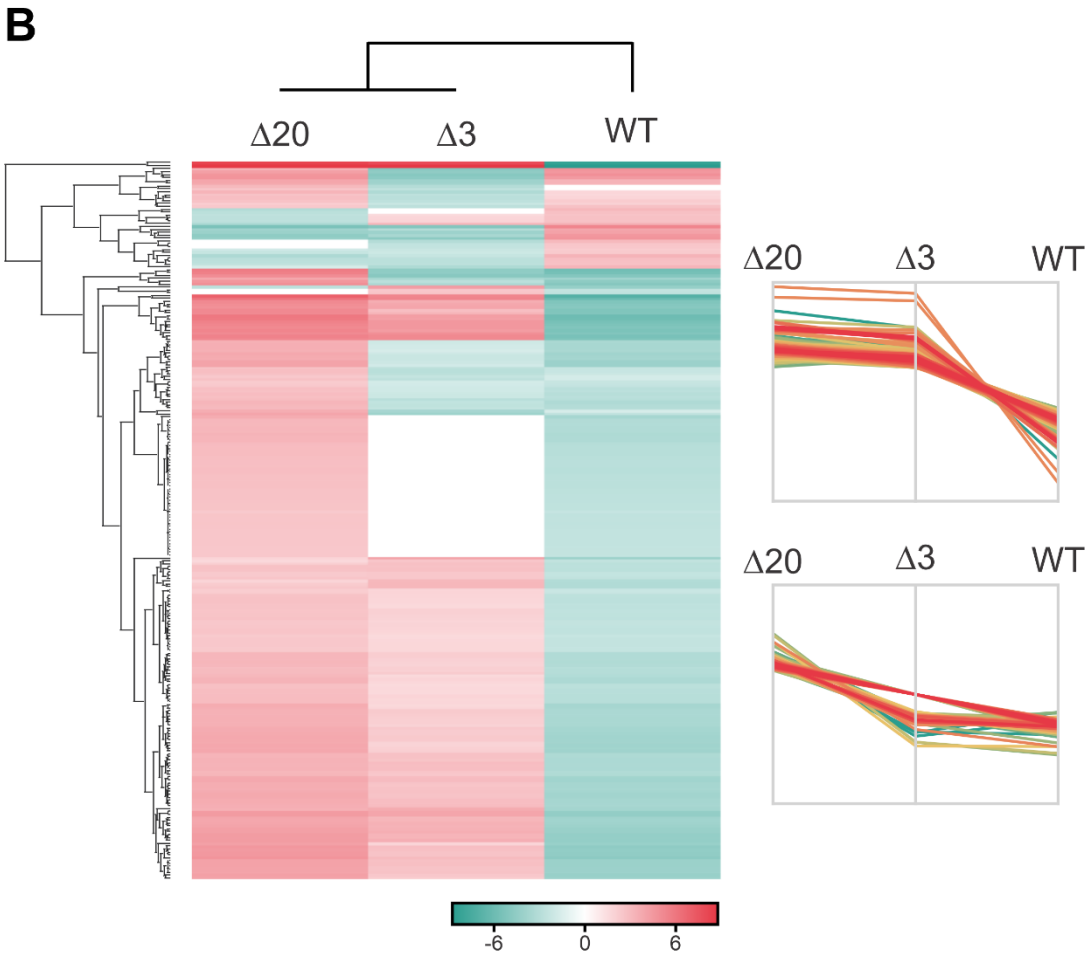
B
Δ20
Δ3
WT
Δ20
Δ3
WT
Δ20
Δ3
WT
-6
0
6

Figure 8. Proteomic responses to the expression of folding-defective FNR variants. (A) UpSet plot with Venn diagram inset showing the number and overlap of differentially expressed proteins in Δ3/WT, Δ20/WT, and Δ20/Δ3 comparisons. Bars represent the size of intersections between sets, with up- and downregulated proteins indicated. The Venn diagram summarizes the overlap of differentially expressed proteins among the three comparisons. (B) Heatmap of significantly regulated proteins across genotypes (Δ20, Δ3, and WT), based on hierarchical clustering. Line plots (right) illustrate representative expression trends for selected clusters, indicating both shared and variant-specific proteomic responses. Two major clusters are depicted: one comprising proteins specifically upregulated in Δ20 and another showing an increase in abundance from WT to Δ3 and Δ20.

Biological interpretation of the proteomics data was aided by network and enrichment analysis. We focused on proteins with significantly increased levels in plants expressing FNR Δ20 and Δ3 compared to controls expressing FNR WT (152 proteins) or those with increased levels only in the FNR Δ20 lines (87 proteins). The Uniprot accession codes for these 239 proteins were used to interrogate the STRING database at a 0.7 confidence threshold. The resulting network was densely connected and presented a few singletons. Enrichment analysis revealed that the term "chloroplast" was significantly enriched, as 50% of the queried proteins were chloroplastic, indicating that half of the proteome variation occurs in this organelle.

Regarding the molecular function of these selected chloroplastic proteins, they are grouped into clusters under the terms "chaperones and proteases," "plastid ribosome," and "photosystems," among others. Chloroplastic chaperones, proteases, and members of the plastid ribosome were detected to have altered levels in response to FNR Δ3 and FNR Δ20. On the other hand, proteins from the photosystems showed altered levels predominantly in response to FNR Δ20 (Figure 9).

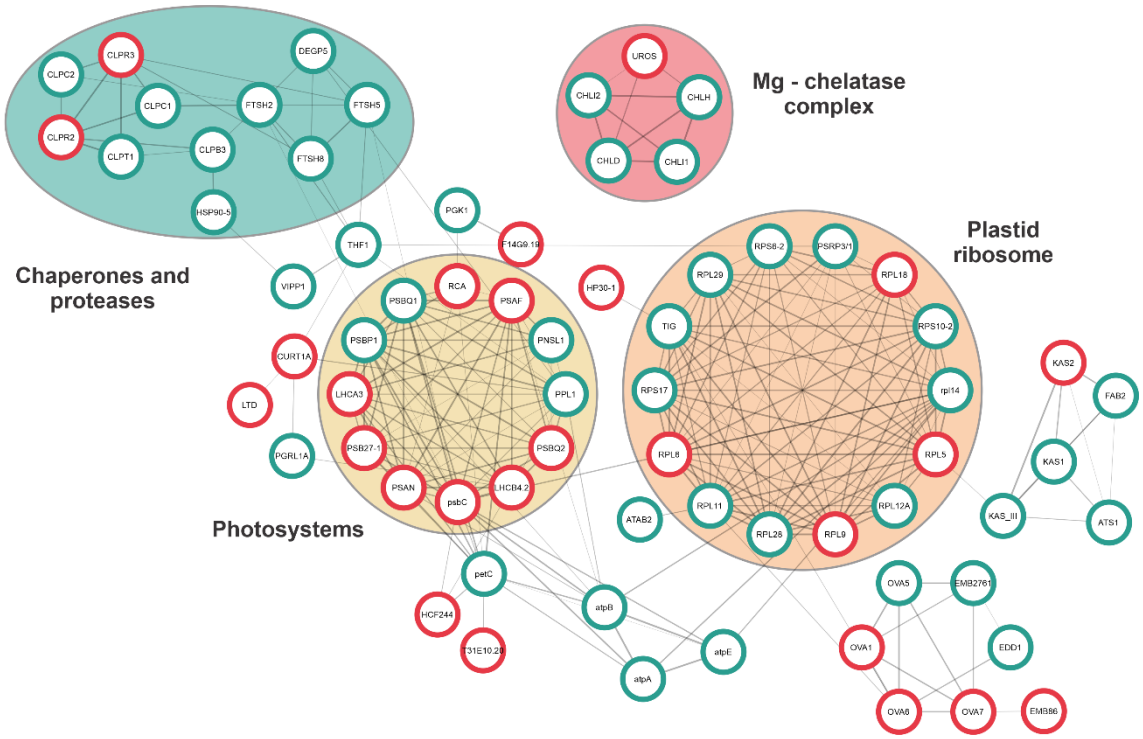

Figure 9: Network and functional enrichment analysis of upregulated proteins in plants expressing folding-defective FNR variants. Protein-protein interaction network generated from 239 proteins upregulated in Δ3 and/or Δ20 lines (STRING confidence ≥ 0.7). Nodes represent individual proteins, with red borders indicating proteins uniquely upregulated in the Δ20 background and blue-green borders denoting proteins upregulated in both Δ3 and Δ20.

Our quantitative proteomics analysis confirmed previous Western blot findings regarding the levels of key chloroplastic chaperones involved in plastidic protein homeostasis. CLPB3 and chloroplastic HSP90C (HSP90-5) displayed increased abundance in both FNR Δ3 and Δ20 overexpressing lines. In contrast, the levels of chloroplastic HSP70s remained unchanged (HSP70.1 and HSP70.2) (Figure 10). The CLP system was also upregulated both in the chaperone complex subunits CLPC1 and CLPC2, as well as with the components of the proteolytic core CLPR2 and CLPR3 and the accessory assembly subunit CLPT1 (Supplementary Table 1). Altogether, the analysis of the expression of these central chaperones and proteases indicates

precise upregulation of the chloroplast proteostasis machinery in response to the expression of FNR Δ3 and Δ20.

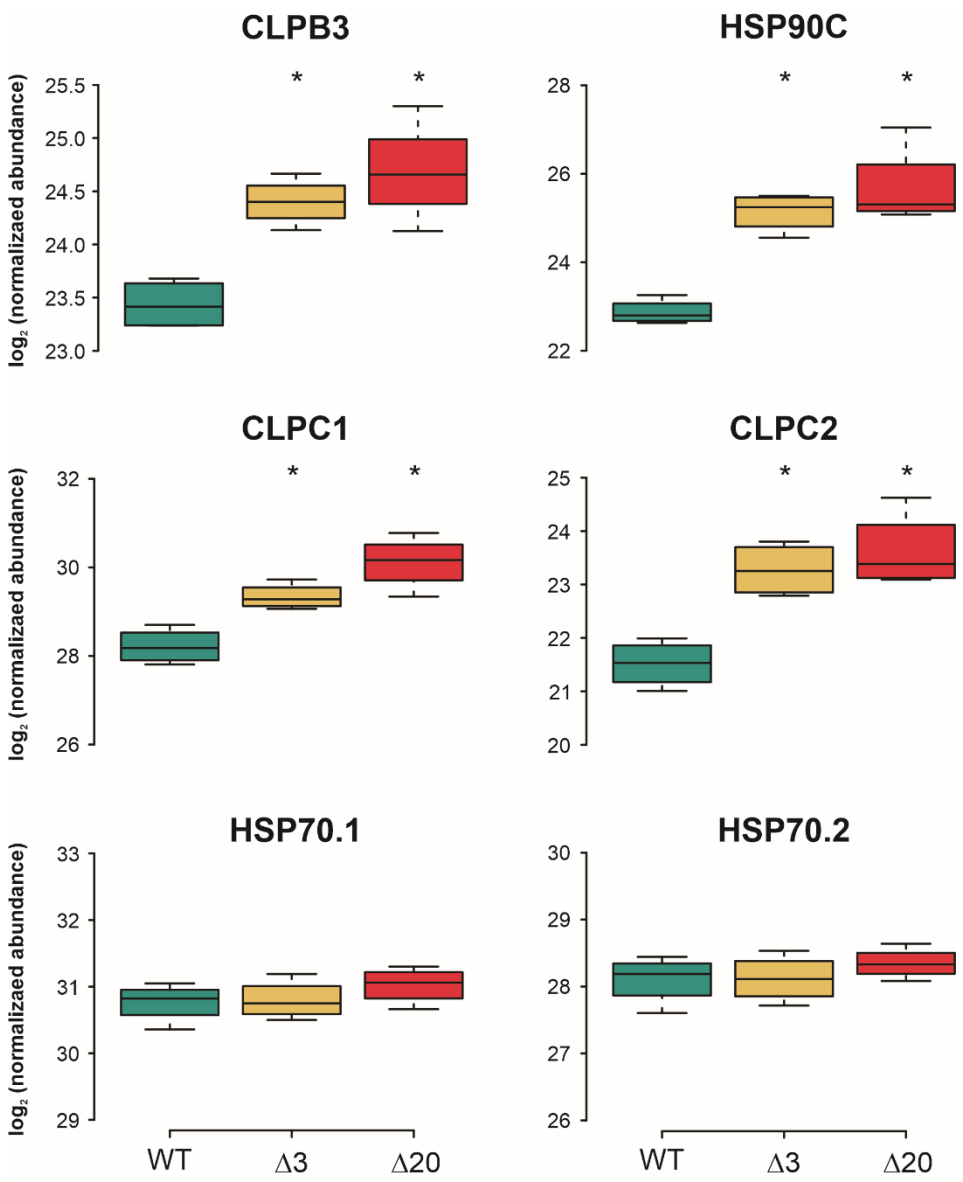

Figure 10. Abundance of selected chloroplastic chaperones in FNR mutant lines. Boxplots showing log2-transformed normalized abundances of CLPB3, CLPC1, CLPC2, HSP90C, HSP70.1, and HSP70.2 in FNR WT, Δ3, and Δ20 backgrounds. Asterisks indicate statistically significant differences ($p < 0.05$) compared to the wild type (WT).

The cpUPR protects plants from thermal stress

Given that most proteins driving changes in the proteome of plants expressing the FNR variants are heat shock proteins and other members of the protein quality control system, we hypothesized that cpUPR activation could prime some tolerance to stress conditions, such as exposure to heat. To this end, plants expressing the FNR variants were subjected to high temperatures (45 ºC, a standard temperature for detecting alterations in plant fitness) and phenotypically inspected. Indeed, plants with an active cpUPR tolerated the treatment: i.e., they continued to grow like controls not subjected to the protocol and displayed less bleaching (Figure 11). Conversely, the growth rate of wild-type plants or those expressing wild-type FNR heated at 45°C was significantly reduced.

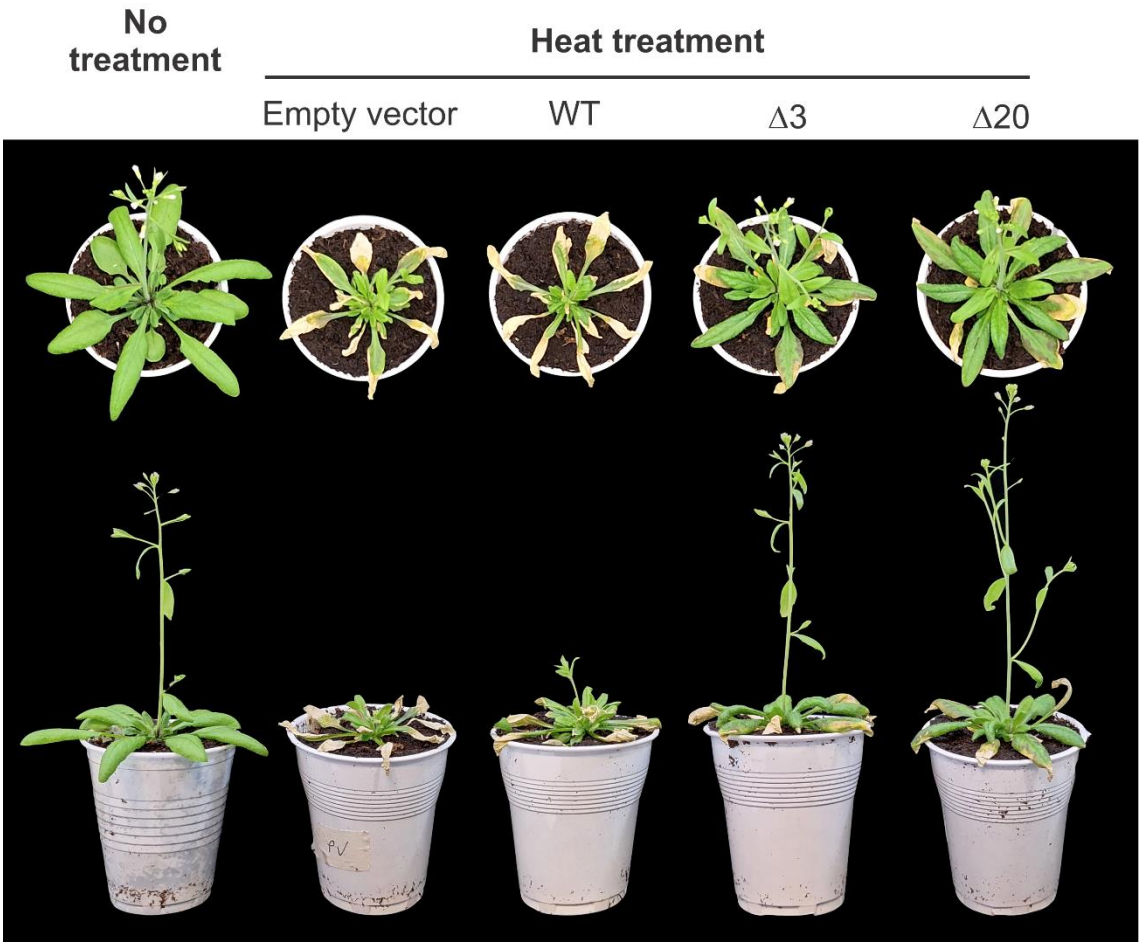

Figure 11: The cpUPR enhances thermotolerance in *Arabidopsis* plants expressing FNR variants. *Arabidopsis* plants expressing wild-type or mutant FNR variants (Δ3 and Δ20) were exposed to heat stress (45 °C) and evaluated for phenotypic responses (n = 4). Top views (upper

row) show bleaching symptoms in rosettes, indicative of heat-induced damage. Side views (lower row) reveal differences in bolting and overall growth. Plants under control conditions (leftmost column) showed normal development across all genotypes.

The proteomic signature of the cpUPR differs from that of the chemically induced UPR.

A large body of evidence for a cpUPR stems from research using plants grown in the presence of LIN and mutants in genes encoding components of the protein quality control (PQC) system (Gao et al., 2023; Llamas & Pulido, 2022). LIN has a dose-dependent effect, ranging from a blockage of plastid expression and accumulation of protein aggregates to a proteotoxic effect as a consequence of perturbation of the import and folding of photosynthetic proteins. In particular, concentrations as high as 550 μm are used to trigger plastidic retrograde signals (Di Silvestre et al., 2025; Koussevitzky et al., 2007; X. Zhao et al., 2018). To discriminate between specific responses caused by the buildup of aggregated proteins (as in *Arabidopsis* lines overexpressing FNR variants) and the broader effect of LIN treatment, we compared these two approaches at a proteomic level. To minimize the deleterious effects of LIN on photosynthetic performance and using ClpB3 levels as a proxy for the imbalance in proteostasis, we selected 15 μM LIN. Under this condition, CLPB3 levels were more than three times higher compared to the controls (Figure 12A). At the same time, the plants exhibited little phenotypic defect, i.e., low chlorosis and smaller size (Figure 12B).

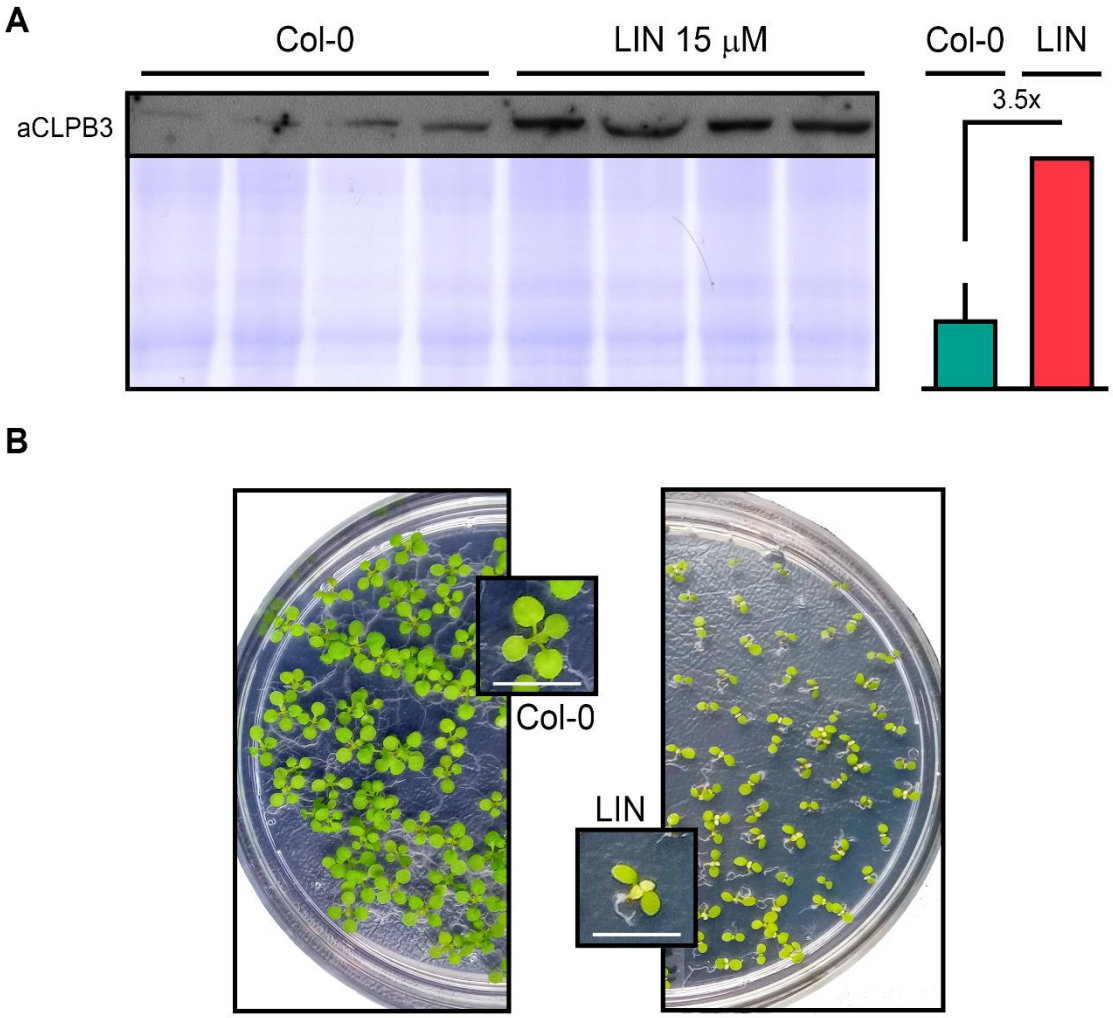

Fig. 12. LIN induces CLPB3 accumulation and some phenotypic alterations in *A. thaliana* seedlings. (A) Immunoblot analysis of CLPB3 levels in 14-day-old *A. thaliana* Col-0 seedlings treated with 15 µM lincomycin (LIN). Total protein extracts were probed with anti-CLPB3 antibodies (top panel), and Coomassie Brilliant Blue staining (bottom panel) was used as a loading control. Bars represent mean ± SD. (B) Representative images showing the phenotypic effects of LIN treatment on *A. thaliana* seedlings. Insets show close-up views of typical individuals from each condition. Scale bars = 5 mm.

Quality control of the proteomics data indicated an excellent correlation between samples and separation of the groups in PCA plots (Figure 13), suggesting changes in the proteome.

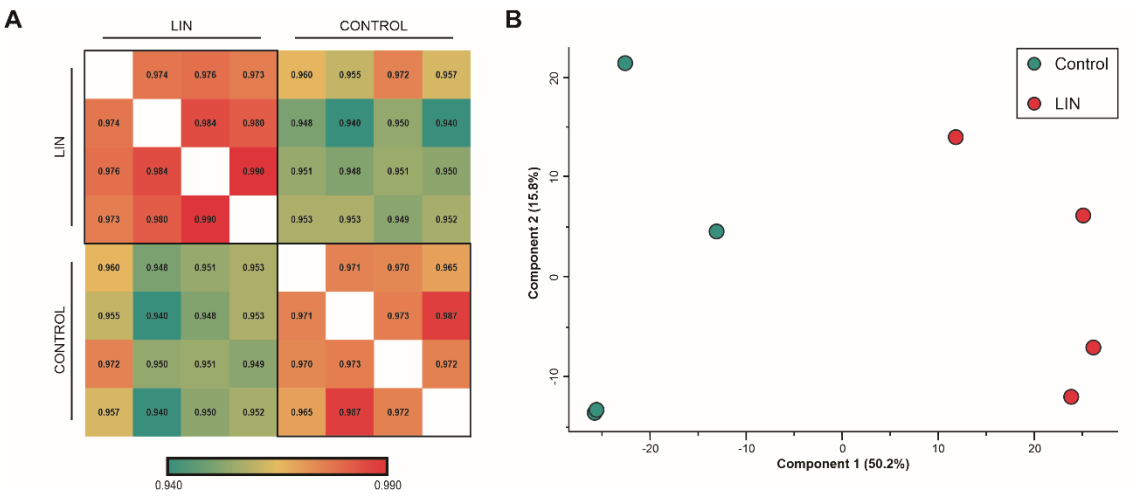

Figure 13. Quality control of proteomics data from LIN-treated and control samples. (A) Pearson correlation heatmap of all biological replicates from LIN-treated and control samples. (B) Principal component analysis of the same datasets shows a clear separation between LIN-treated (red) and control (blue-green) samples along the first principal component (PC1, 50.2%).

However, the set of proteins with altered abundance in seedlings treated with 15 µM LIN differed markedly from those observed in plants expressing the aggregation-prone FNR variants. Among the chloroplast-localized quality control proteins, only CLPB3 and FTSH8 showed an increase in abundance approaching twofold. In contrast, most chaperones and proteases upregulated in the FNR variant-expressing plants showed minimal changes or fell below the significance threshold in LIN-treated samples (Figure 14).

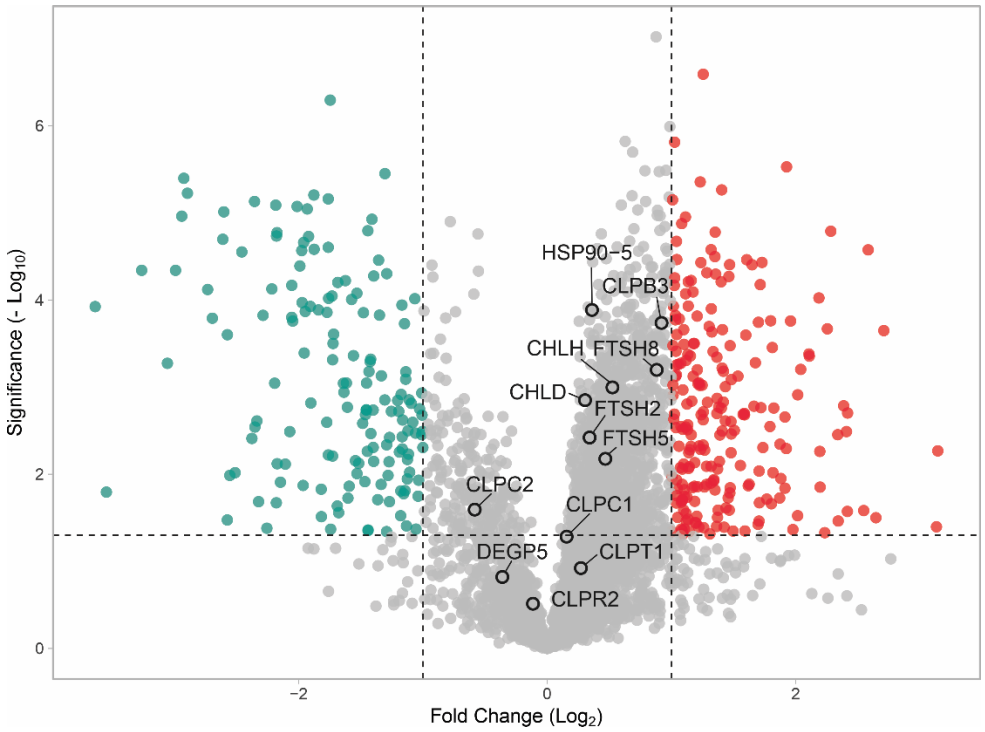

Figure 14. Differential protein abundance in LIN-treated *A. thaliana* seedlings. Volcano plot showing changes in protein abundance in 14-day-old Col-0 seedlings treated with 15 µM lincomycin (LIN) compared to untreated controls. Proteins significantly upregulated (red) or downregulated (blue-green) are shown, based on thresholds of ($\log_2$ fold change) > 1 and adjusted $p < 0.05$ (dashed lines). Highlighted proteins include chloroplast-localized chaperones and proteases.

Proteins with significantly elevated levels were loosely connected, and singletons were abundant. There were no enriched Gene Ontology terms for this group. Proteins with considerably lower levels formed an extensive network comprising two major clusters: ribosomal proteins and proteins involved in photosynthesis (Figure 15 and Supplementary Table 2). The overall comparison between FNR variants- and LIN-triggered UPR reveals two types of response. LIN-treated plants showed a slight increase in levels of PQC members while broadly repressing plastid gene expression and downregulation of photosynthetic proteins. In contrast,

the response to the presence of FNR Δ3 and FNR Δ20 contributed differently to restoring proteostasis by inducing a more complex set of PQC components and enhancing plastid gene expression, ultimately improving chloroplast functionality under this condition.

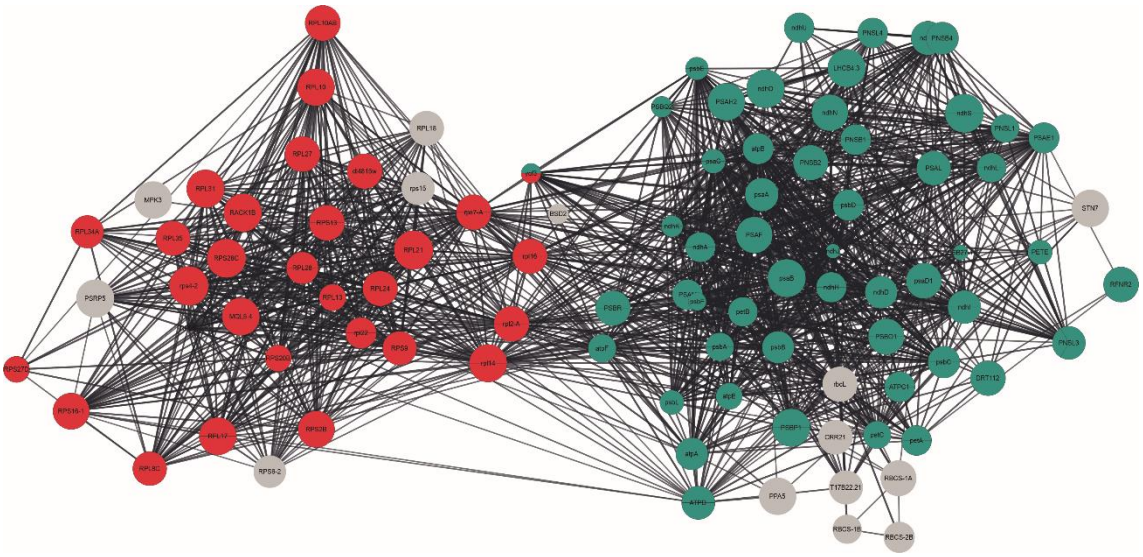

Figure 15: Interaction network of downregulated proteins in LIN-treated seedlings. Proteins with lowered abundances in response to 15 µM LIN treatment were mapped using STRING interaction data. Downregulated proteins (log_2 fold change ≤ –1; node size reflects magnitude) formed a highly interconnected network with two major clusters: ribosomal proteins (red nodes) and proteins associated with photosynthesis (blue-green nodes).

DISCUSSION

Over the last decade, numerous lines of research have pointed out an unfolded protein response in chloroplasts using several strategies like mutants in PQC components and LIN treatments (Dogra et al., 2019; Llamas et al., 2017; Ramundo & Rochaix, 2014a and reviewed in Gao et al., 2023; Llamas & Pulido, 2022). To add definitive evidence for its existence, we drew inspiration

from earlier work in mitochondria and the ER, where the buildup of aggregation-prone proteins unleashed the corresponding UPR. In this way, the overlap of responses induced by global triggers (such as chemicals and abiotic stress) is diminished, and the molecular actors of the UPR can thus be uncovered. We chose variants of FNR that our group designed and characterized more than 30 years ago (Orellano et al., 1993). Three or twenty residues were eliminated from the C-terminal end, preventing proper folding. As evidenced by mass spectrometry identification and fluorescence microscopy, the reductases were expressed in leaves and accumulated in chloroplasts. This was expected, at least, for the wild-type protein, as transgenic tobacco plants overexpressing pea FNR had already been reported. As described by Rodriguez et al., the overexpression of pea FNR does not affect growth or photosynthetic parameters under normal conditions (Rodriguez et al., 2007). However, the accumulation of FNR WT was several times higher than that of the folding defective variants, even though all genetic constructs used for plant transformation were the same. This suggests prompt degradation of the misfolded variants as part of a functional proteostatic response, in line with the increase in protease content of the chloroplast.

The induction of *A. thaliana* CLPB3 and CLPC in the presence of the FNRs variants was part of a more complex response to restore proteostasis. Proteomic analysis revealed a coordinated increase of chaperones, proteases, and accessory assembly factors of the PQC system in response to FNR Δ3 and Δ20. FTSH is an ATP-dependent zinc metalloprotease complex anchored in the thylakoid membrane, comprised of four major isoforms (1, 2, 5, and 8) (Van Wijk, 2024). Higher amounts of FTSH 2, 5, and 8 were detected in FNR Δ3 and Δ20 overexpressing plants compared to overexpression of wild-type FNR. Another induced plastidic protease was DEG5, belonging to the DEG protease (formerly DEGP), which are ATP-independent Ser-type endopeptidases in the thylakoid lumen and stroma. These protease complexes are central for chloroplast proteostasis, and they act together to degrade photodamaged D1 subunits of the PSII reaction center (reviewed in (Yoshioka-Nishimura & Yamamoto, 2014). We also observed a

substantial accumulation of components of the stromal CLP protease. None of these proteases usually degrade appropriately folded proteins. Therefore, they are presented with substrates that adaptors and molecular chaperones have previously recognized (Aguilar Lucero et al., 2021; Rosano et al., 2012). For example, CLPC1 and C2 are HSP100 hexameric chaperones that unfold damaged proteins and translocate them through their central pore to the barrel-shaped CLPP protease (Bruch et al., 2012; Rosano et al., 2011). Levels of both CLPC1 and C2 were increased in *A. thaliana* plants overexpressing the folding-defective FNR variants. The abundance of the assembly protein CLPT1 (Colombo et al., 2014; Kim et al., 2015) and the proteolytic subunits CLPR2 and CLPR3 increased as well (Kim et al., 2009). The ultimate fate of a misfolded protein is not always degradation; a subset of chaperones also rescue them from aggregates and partially folded intermediates. The major chloroplastic disaggregase is CLPB3, which can refold aggregated proteins *in vitro* (Parcerisa et al., 2020). HSP90.5 is vital for chloroplast biogenesis and embryogenesis, while its interaction partner VIPP1 is essential for the biogenesis and maintenance of thylakoid membranes (Feng et al., 2014). These three proteins showed higher levels in response to FNR Δ3 and Δ20, underscoring the molecular response to their presence. Based on these results, our proteomic analysis of the leaf proteome in the presence of FNR Δ3 and Δ20 provides a *bona fide* description of an activated cpUPR to sustain proteostasis.

Most components of the chloroplast quality control system are encoded in the nucleus, implying that their induction relies on retrograde signals from the organelle to the nucleus to restore proteostasis (Barajas-López et al., 2013; Gao et al., 2023). Mounting evidence highlights GUN1 as an important, albeit indirect, regulator of chloroplast stress responses (Gao et al., 2023; Llamas & Pulido, 2022; Wu & Bock, 2021). GUN1 is a pentatricopeptide repeat-containing protein that integrates multiple retrograde signaling pathways (Wu & Bock, 2021). During early plant development, it represses photosynthesis-associated nuclear gene expression in response to plastid dysfunction, particularly upon treatment with inhibitors such as LIN or norfluorazon, the latter triggering plastid gene expression pathways through photooxidative damage

(Koussevitzky et al., 2007; Wu et al., 2018; Wu, Meyer, Wu, et al., 2019; X. Zhao et al., 2018). Mutants impaired in plastid gene expression or PQC components often display plastid-dependent phenotypes (e.g., pale or variegated leaves) that are suppressed by loss of GUN1 function, further implicating GUN1 in stress-related retrograde signaling (Gao et al., 2023; Marino et al., 2019; Tadini et al., 2016, 2020; Wu, Meyer, Wu, et al., 2019).

In our proteomic analysis, GUN1 was not detected in plants expressing FNR Δ3, Δ20, or treated with LIN. Although this prevents concluding its role in the cpUPR, several factors may explain its absence. First, our experiments were performed in 14-day-old *Arabidopsis* seedlings, a stage when GUN1 is post-transcriptionally repressed (Wu et al., 2018). Second, the strong induction of CLPC1 and CLPC2 in response to the FNR variants may promote GUN1 degradation, as previously reported (Wu et al., 2018). Third, both GUN1 levels and the severity of the *gun* phenotype depend on the intensity and timing of chloroplast stress (Llamas et al., 2017; Tadini et al., 2020; Wu et al., 2018; X. Zhao et al., 2018). The mild LIN treatment used here (15 µM) likely contributes to the lack of GUN1 detection yet still impairs chloroplast function by suppressing photosynthetic gene expression and protein import. In contrast, in our FNR variants model, the degree of proteotoxic effect is so gentle that the cpUPR can be activated and studied in phenotypically normal seedlings, offering a more nuanced view of the organelle's ability to communicate and recover from the imbalance of the proteostasis.

Interestingly, together with the general induction of photosynthetic genes (see below), we observed an increase in the enzymes of tetrapyrrole biosynthesis. GUN5 (ChlH), as well as all of the Mg-chelatase complex subunits, showed increased levels in plants overexpressing the folding-defective FNRs. The complex plays a fundamental role in chlorophyll biosynthesis by catalyzing the insertion of a magnesium ion into protoporphyrin IX. This commits the precursor to chlorophyll biosynthesis, a pathway essential for producing the pigment. Beyond its enzymatic role, the Mg-chelatase complex, particularly its ChlH (GUN5) subunit, is involved in

plastid-to-nucleus retrograde signaling (Mochizuki et al., 2001; Wang et al., 2023), although the intermediate steps of the mechanism are not fully understood (Kindgren et al., 2012; Strand et al., 2003; Wang et al., 2023). Our results suggest an increase in the tetrapyrrole biosynthesis pathway, which might contribute to cpUPR-related gene expression.

In our work, the cpUPR was triggered by the expression of folding-defective proteins targeted to chloroplasts, drawing inspiration from the work of Zhao et al. that used a truncated version of OTC to unleash the mitochondrial UPR (Q. Zhao et al., 2002). Moreover, we used two variants with different solubility, permitting us to unveil the molecular players of the cpUPR as the protein crisis gets more severe. Overexpressing FNR Δ3 and Δ20 increases chloroplastic chaperones and proteases. However, FNR Δ20 adds a new layer of complexity, comprising proteins involved in membrane remodeling and further protection against stress. For example, SLOW GREEN 1 (SG1) is required for the early stage of chloroplast development. It may be involved in chloroplast protein biosynthesis and/or degradation (Hu et al., 2014). Photosystem II repair protein PSB27-H1 is engaged in the repair of photodamaged photosystem II (Nowaczyk et al., 2006). Protein CURVATURE THYLAKOID 1A determines thylakoid architecture by inducing membrane curvature (Armbruster et al., 2013). Protein HIGH CHLOROPHYLL FLUORESCENCE PHENOTYPE 244 is required for the biogenesis of photosystem II, especially for synthesizing the reaction center proteins (e.g., D1) (Li et al., 2019). Considering the functions of the proteins, we can speculate that the cpUPR is a mechanism to protect the photosynthetic chain. As proteins involved in photosynthesis are damage-prone, the organelle interprets the presence of aggregates as a general signal of injury, particularly damning to the photosynthetic electron transport chain.

Our comparative proteomic analysis of the stress response triggered by overexpressing the FNR variants and LIN shows that, while these processes share certain features, they also exhibit significant differences. CLPB3 and HSP90-5 showed increased levels under both treatments

(although both were slightly below our chosen two-fold threshold in the proteomic analysis of plants under LIN treatment), which agrees with other reports using 15 μM LIN (Llamas et al., 2017). However, there was little overlap in the molecular response to low concentrations of LIN compared to our strategy. LIN treatment negatively impacted photosynthetic proteins and the plastid ribosome. Yet, its effect on chaperones, proteases, and other members of the PQC network was low. Strikingly, the levels of photosynthetic proteins showed opposite trends. Under LIN treatment, their abundance lowered, but a significant increase was detected in plants overexpressing the FNR variants. The former effect was expected as LIN causes chlorosis and disruption of the photosynthetic electron transport chain, leading to the degradation of its constituents. Building upon our hypothesis that the accumulation of the FNR variants is sensed as stress akin to high light or thermal insults (which mainly affect the electron transport chain), the upregulation of photosynthetic proteins may be a mechanism for their rapid replenishment to ensure proteostasis.

The striking upregulation of members of the quality control systems in response to the folding-defective FNRs prompted us to analyze whether these plants were better equipped to endure environmental stress. This was the case: plants overexpressing FNR Δ3 or Δ20 were more heat tolerant than controls. As the cpUPR was permanently activated, it likely protected the plants from severe protein damage. Creating stress-tolerant plants by overexpressing a given protein in chloroplasts is a common strategy in agrobiotechnology (Nouri & Komatsu, 2013). The fitness of transgenic organisms is typically compared to that of wild-type plants or empty vector controls. However, it is rarely assessed whether the overexpressed protein is correctly folded. This raises the possibility that stress tolerance observed in transgenic plants may, at least in part, result from the activation of a UPR rather than the specific function of the protein itself. In this context, tolerance attributed to the biological activity of a foreign protein might instead arise from its misfolding or its overaccumulation beyond the folding capacity of the host cell.

In conclusion, targeting folding defective proteins to the chloroplast, as has been done for other compartments, allowed us to provide direct evidence for the cpUPR and identify part of its molecular components. Unlike traditional cpUPR models reliant on global stress or pleiotropic inhibitors, our strategy offers more control over the nature and severity of proteostatic stress within the chloroplast. This not only reveals key components of the cpUPR but opens a path for broader applications in organellar biology and stress-resilient plant design.

ACKNOWLEDGMENTS

We thank Dr. Enrique Morales for technical support in confocal microscopy. This work was supported with a grant from the Agencia Nacional de Promoción de la Investigación, el Desarrollo Tecnológico y la Innovación (PICT 2019-02971) awarded to GLR.

REFERENCES

Aguilar Lucero, D., Cantoia, A., Sánchez-López, C., Binolfi, A., Mogk, A., Ceccarelli, E. A., & Rosano, G. L. (2021). Structural features of the plant N-recognin ClpS1 and sequence determinants in its targets that govern substrate selection. FEBS Letters, 595(11). https://doi.org/10.1002/1873-3468.14081

Almagro Armenteros, J. J., Salvatore, M., Emanuelsson, O., Winther, O., Von Heijne, G., Elofsson, A., & Nielsen, H. (2019). Detecting sequence signals in targeting peptides using deep learning. Life Science Alliance, 2(5), e201900429. https://doi.org/10.26508/lsa.201900429

Armbruster, U., Labs, M., Pribil, M., Viola, S., Xu, W., Scharfenberg, M., Hertle, A. P., Rojahn, U., Jensen, P. E., Rappaport, F., Joliot, P., Dormann, P., Wanner, G., & Leister, D. (2013). Arabidopsis CURVATURE THYLAKOID1 Proteins Modify Thylakoid Architecture by Inducing Membrane Curvature. The Plant Cell, 25(7), 2661-2678. https://doi.org/10.1105/tpc.113.113118

Barajas-López, J. D. D., Blanco, N. E., & Strand, Å. (2013). Plastid-to-nucleus communication, signals controlling the running of the plant cell. Biochimica et Biophysica Acta (BBA) - Molecular Cell Research, 1833(2), 425-437. https://doi.org/10.1016/j.bbamcr.2012.06.020

Bergmann, T. J., Fregno, I., Fumagalli, F., Rinaldi, A., Bertoni, F., Boersema, P. J., Picotti, P., & Molinari, M. (2018). Chemical stresses fail to mimic the unfolded protein response resulting from luminal load with unfolded polypeptides. Journal of Biological Chemistry, 293(15), 5600-5612. https://doi.org/10.1074/jbc.RA117.001484

Bergmann, T. J., & Molinari, M. (2018). Three branches to rule them all? UPR signalling in response to chemically versus misfolded proteins-induced ER stress: Chemical ER stress versus misfolded protein-induced ER stress. Biology of the Cell, 110(9), 197-204. https://doi.org/10.1111/boc.201800029

Blanco, N. E., Liebsch, D., Guinea Díaz, M., Strand, Å., & Whelan, J. (2019). Dual and dynamic intracellular localization of Arabidopsis thaliana SnRK1.1. Journal of Experimental Botany, 70(8), 2325-2338. https://doi.org/10.1093/jxb/erz023

Braakman, I., Helenius, J., & Helenius, A. (1992). Manipulating disulfide bond formation and protein folding in the endoplasmic reticulum. The EMBO Journal, 11(5), 1717-1722. https://doi.org/10.1002/j.1460-2075.1992.tb05223.x

Bruch, E. M., Rosano, G. L., & Ceccarelli, E. A. (2012). Chloroplastic Hsp100 chaperones ClpC2 and ClpD interact in vitro with a transit peptide only when it is located at the N-terminus of a protein. BMC Plant Biology, 12. https://doi.org/10.1186/1471-2229-12-57

Chapman, R., Sidrauski, C., & Walter, P. (1998). Intracellular signaling from the endoplasmic reticulum to the nucleus. Annual Review of Cell and Developmental Biology, 14(1), 459-485. https://doi.org/10.1146/annurev.cellbio.14.1.459

Clough, S. J., & Bent, A. F. (1998). Floral dip: A simplified method for Agrobacterium -mediated transformation of Arabidopsis thaliana . The Plant Journal, 16(6), 735-743. https://doi.org/10.1046/j.1365-313x.1998.00343.x

Colombo, C. V., Ceccarelli, E. A., & Rosano, G. L. (2014). Characterization of the accessory protein ClpT1 from Arabidopsis thaliana: Oligomerization status and interaction with Hsp100 chaperones. BMC Plant Biology, 14(1). https://doi.org/10.1186/s12870-014-0228-0

Di Silvestre, D., Jeran, N., Domingo, G., Vannini, C., Marsoni, M., Fortunato, S., De Pinto, M. C., Tamborrino, A., Negroni, Y. L., Zottini, M., Hong, L. T., Lomagno, A., Mauri, P., Pesaresi, P., & Tadini, L. (2025). A Holistic Investigation of Arabidopsis Proteomes Altered in Chloroplast Biogenesis and Retrograde Signalling Identifies PsbO as a Key Regulator of Chloroplast Quality Control. Plant, Cell & Environment, pce.15611. https://doi.org/10.1111/pce.15611

Dogra, V., Duan, J., Lee, K. P., & Kim, C. (2019). Impaired PSII proteostasis triggers a UPR-like response in the var2 mutant of Arabidopsis. Journal of Experimental Botany, 70(12). https://doi.org/10.1093/jxb/erz151

Feng, J., Fan, P., Jiang, P., Lv, S., Chen, X., & Li, Y. (2014). Chloroplast-targeted Hsp90 plays essential roles in plastid development and embryogenesis in Arabidopsis possibly linking with VIPP1. Physiologia Plantarum, 150(2), 292-307. https://doi.org/10.1111/ppl.12083

Gao, L.-L., Hong, Z.-H., Wang, Y., & Wu, G.-Z. (2023). Chloroplast proteostasis: A story of birth, life, and death. Plant Communications, 4(1), 100424. https://doi.org/10.1016/j.xplc.2022.100424

Gopakumar, G., & Singh, J. (2022). Dithiothreitol causes toxicity in C. elegans by modulating the methionine–homocysteine cycle. eLife, 11, e76021. https://doi.org/10.7554/eLife.76021

Heifetz, A., Keenan, R. W., & Elbein, A. D. (1979). Mechanism of action of tunicamycin on the UDP-GlcNAc:dolichyl-phosphate GlcNAc-1-phosphate transferase. Biochemistry, 18(11), 2186-2192. https://doi.org/10.1021/bi00578a008

Hetz, C. (2012). The unfolded protein response: Controlling cell fate decisions under ER stress and beyond. Nature Reviews Molecular Cell Biology, 13(2), 89-102. https://doi.org/10.1038/nrm3270

Hidvegi, T., Schmidt, B. Z., Hale, P., & Perlmutter, D. H. (2005). Accumulation of Mutant α1-Antitrypsin Z in the Endoplasmic Reticulum Activates Caspases-4 and -12, NFκB, and BAP31 but Not the Unfolded Protein Response. Journal of Biological Chemistry, 280(47), 39002-39015. https://doi.org/10.1074/jbc.M508652200

Hoogenraad, N. (2017). A brief history of the discovery of the mitochondrial unfolded protein response in mammalian cells. Journal of Bioenergetics and Biomembranes, 49(4), 293-295. https://doi.org/10.1007/s10863-017-9703-2

Hu, Z., Xu, F., Guan, L., Qian, P., Liu, Y., Zhang, H., Huang, Y., & Hou, S. (2014). The tetratricopeptide repeat-containing protein slow green1 is required for chloroplast development in Arabidopsis. Journal of Experimental Botany, 65(4), 1111-1123. https://doi.org/10.1093/jxb/ert463

Kato, Y., Sun, X., Zhang, L., & Sakamoto, W. (2012). Cooperative D1 Degradation in the Photosystem II Repair Mediated by Chloroplastic Proteases in Arabidopsis. Plant Physiology, 159(4), 1428-1439. https://doi.org/10.1104/pp.112.199042

Kim, J., Kimber, M. S., Nishimura, K., Friso, G., Schultz, L., Ponnala, L., & van Wijka, K. J. (2015). Structures, functions, and interactions of ClpT1 and ClpT2 in the Clp protease system of arabidopsis chloroplasts. Plant Cell, 27(5). https://doi.org/10.1105/tpc.15.00106

Kim, J., Rudella, A., Ramirez Rodriguez, V., Zybailov, B., Olinares, P. D. B., & Van Wijk, K. J. (2009). Subunits of the Plastid ClpPR Protease Complex Have Differential Contributions to Embryogenesis, Plastid Biogenesis, and Plant Development in Arabidopsis. The Plant Cell, 21(6), 1669-1692. https://doi.org/10.1105/tpc.108.063784

Kindgren, P., Norén, L., Barajas López, J. D. D., Shaikhali, J., & Strand, Å. (2012). Interplay between HEAT SHOCK PROTEIN 90 and HY5 Controls PhANG Expression in Response to the GUN5 Plastid Signal. Molecular Plant, 5(4), 901-913. https://doi.org/10.1093/mp/ssr112

Koussevitzky, S., Nott, A., Mockler, T. C., Hong, F., Sachetto-Martins, G., Surpin, M., Lim, J., Mittler, R., & Chory, J. (2007). Signals from chloroplasts converge to regulate nuclear gene expression. Science (New York, N.Y.), 316(5825), 715-719.

Kozutsumi, Y., Segal, M., Normington, K., Gething, M.-J., & Sambrook, J. (1988). The presence of malfolded proteins in the endoplasmic reticulum signals the induction of glucose-regulated proteins. Nature, 332(6163), 462-464. https://doi.org/10.1038/332462a0

Li, Y., Liu, B., Zhang, J., Kong, F., Zhang, L., Meng, H., Li, W., Rochaix, J.-D., Li, D., & Peng, L. (2019). OHP1, OHP2, and HCF244 Form a Transient Functional Complex with the Photosystem II Reaction Center. Plant Physiology, 179(1), 195-208. https://doi.org/10.1104/pp.18.01231

Llamas, E., & Pulido, P. (2022). A proteostasis network safeguards the chloroplast proteome. Essays in Biochemistry, 66(2), 219-228. https://doi.org/10.1042/EBC20210058

Llamas, E., Pulido, P., & Rodriguez-Concepcion, M. (2017). Interference with plastome gene expression and Clp protease activity in Arabidopsis triggers a chloroplast unfolded protein response to restore protein homeostasis. PLoS Genetics, 13(9). https://doi.org/10.1371/journal.pgen.1007022

Marino, G., Naranjo, B., Wang, J., Penzler, J., Kleine, T., & Leister, D. (2019). Relationship of GUN 1 to FUG 1 in chloroplast protein homeostasis. The Plant Journal, 99(3), 521-535. https://doi.org/10.1111/tpj.14342

Metzger, M. B., & Michaelis, S. (2009). Analysis of Quality Control Substrates in Distinct Cellular Compartments Reveals a Unique Role for Rpn4p in Tolerating Misfolded Membrane Proteins. Molecular Biology of the Cell, 20(3), 1006-1019. https://doi.org/10.1091/mbc.e08-02-0140

Mochizuki, N., Brusslan, J. A., Larkin, R., Nagatani, A., & Chory, J. (2001). Arabidopsis genomes uncoupled 5 (GUN5) mutant reveals the involvement of Mg-chelatase H subunit in plastid-to-nucleus signal transduction. Proceedings of the National Academy of Sciences, 98(4), 2053-2058. https://doi.org/10.1073/pnas.98.4.2053

Mogk, A., Bukau, B., & Kampinga, H. H. (2018). Cellular Handling of Protein Aggregates by Disaggregation Machines. Molecular Cell, 69(2), 214-226. https://doi.org/10.1016/j.molcel.2018.01.004

Mulo, P., Pursiheimo, S., Hou, C.-X., Tyystjärvi, T., & Aro, E.-M. (2003). Multiple effects of antibiotics on chloroplast and nuclear gene expression. Functional Plant Biology, 30(11), 1097. https://doi.org/10.1071/FP03149

Münch, C., & Harper, J. W. (2016). Mitochondrial unfolded protein response controls matrix pre-RNA processing and translation. Nature, 534(7609), 710-713. https://doi.org/10.1038/nature18302

Nouri, M.-Z., & Komatsu, S. (2013). Subcellular protein overexpression to develop abiotic stress tolerant plants. Frontiers in Plant Science, 4. https://doi.org/10.3389/fpls.2013.00002

Nowaczyk, M. M., Hebeler, R., Schlodder, E., Meyer, H. E., Warscheid, B., & Rögner, M. (2006). Psb27, a Cyanobacterial Lipoprotein, Is Involved in the Repair Cycle of Photosystem II. The Plant Cell, 18(11), 3121-3131. https://doi.org/10.1105/tpc.106.042671

Orellano, E. G., Calcaterra, N. B., Carrillo, N., & Ceccarelli, E. A. (1993). Probing the role of the carboxyl-terminal region of ferredoxin-NADP+ reductase by site-directed mutagenesis and deletion analysis. Journal of Biological Chemistry, 268(26), 19267-19273. https://doi.org/10.1016/S0021-9258(19)36509-3

Parcerisa, I. L., Rosano, G. L., & Ceccarelli, E. A. (2020). Biochemical characterization of ClpB3, a chloroplastic disaggregase from Arabidopsis thaliana. Plant Molecular Biology, 104(4-5). https://doi.org/10.1007/s11103-020-01050-7

Perez-Riverol, Y., Bandla, C., Kundu, D. J., Kamatchinathan, S., Bai, J., Hewapathirana, S., John, N. S., Prakash, A., Walzer, M., Wang, S., & Vizcaíno, J. A. (2025). The PRIDE database at 20 years: 2025 update. Nucleic Acids Research, 53(D1), D543-D553. https://doi.org/10.1093/nar/gkae1011

Ramundo, S., & Rochaix, J. D. (2014a). Chloroplast unfolded protein response, a new plastid stress signaling pathway? Plant Signaling and Behavior, 9(10). https://doi.org/10.4161/15592316.2014.972874

Ramundo, S., & Rochaix, J. D. (2014b). Loss of chloroplast ClpP elicits an autophagy-like response in Chlamydomonas. Autophagy, 10(9). https://doi.org/10.4161/auto.29960

Read, A., & Schröder, M. (2021). The Unfolded Protein Response: An Overview. Biology, 10(5), 384. https://doi.org/10.3390/biology10050384

Rodriguez, R. E., Lodeyro, A., Poli, H. O., Zurbriggen, M., Peisker, M., Palatnik, J. F., Tognetti, V. B., Tschiersch, H., Hajirezaei, M.-R., Valle, E. M., & Carrillo, N. (2007). Transgenic Tobacco Plants

Overexpressing Chloroplastic Ferredoxin-NADP(H) Reductase Display Normal Rates of Photosynthesis and Increased Tolerance to Oxidative Stress. Plant Physiology, 143(2), 639-649. https://doi.org/10.1104/pp.106.090449

Rosano, G. L., Bruch, E. M., & Ceccarelli, E. A. (2011). Insights into the CLP/HSP100 chaperone system from chloroplasts of Arabidopsis thaliana. Journal of Biological Chemistry, 286(34). https://doi.org/10.1074/jbc.M110.211946

Rosano, G. L., Bruch, E. M., Colombo, C. V., & Ceccarelli, E. A. (2012). Toward a unified model of the action of CLP/HSP100 chaperones in chloroplasts. Plant Signaling and Behavior, 7(6). https://doi.org/10.4161/psb.19992

Ruckle, M. E., Burgoon, L. D., Lawrence, L. A., Sinkler, C. A., & Larkin, R. M. (2012). Plastids Are Major Regulators of Light Signaling in Arabidopsis. Plant Physiology, 159(1), 366-390. https://doi.org/10.1104/pp.112.193599

Schindelin, J., Arganda-Carreras, I., Frise, E., Kaynig, V., Longair, M., Pietzsch, T., Preibisch, S., Rueden, C., Saalfeld, S., Schmid, B., Tinevez, J.-Y., White, D. J., Hartenstein, V., Eliceiri, K., Tomancak, P., & Cardona, A. (2012). Fiji: An open-source platform for biological-image analysis. Nature Methods, 9(7), 676-682. https://doi.org/10.1038/nmeth.2019

Shpilka, T., & Haynes, C. M. (2018). The mitochondrial UPR: Mechanisms, physiological functions and implications in ageing. Nature Reviews Molecular Cell Biology, 19(2), 109-120. https://doi.org/10.1038/nrm.2017.110

Strand, Å., Asami, T., Alonso, J., Ecker, J. R., & Chory, J. (2003). Chloroplast to nucleus communication triggered by accumulation of Mg-protoporphyrinIX. Nature, 421(6918), 79-83. https://doi.org/10.1038/nature01204

Tadini, L., Peracchio, C., Trotta, A., Colombo, M., Mancini, I., Jeran, N., Costa, A., Faoro, F., Marsoni, M., Vannini, C., Aro, E., & Pesaresi, P. (2020). GUN1 influences the accumulation of NEP-dependent transcripts and chloroplast protein import in Arabidopsis cotyledons upon perturbation of chloroplast protein homeostasis. The Plant Journal, 101(5), 1198-1220. https://doi.org/10.1111/tpj.14585

Tadini, L., Pesaresi, P., Kleine, T., Rossi, F., Guljamow, A., Sommer, F., Mühlhaus, T., Schroda, M., Masiero, S., Pribil, M., Rothbart, M., Hedtke, B., Grimm, B., & Leister, D. (2016). GUN1 Controls Accumulation of the Plastid Ribosomal Protein S1 at the Protein Level and Interacts with Proteins Involved in Plastid Protein Homeostasis. Plant Physiology, 170(3), 1817-1830. https://doi.org/10.1104/pp.15.02033

Tyanova, S., Temu, T., Sinitcyn, P., Carlson, A., Hein, M. Y., Geiger, T., Mann, M., & Cox, J. (2016). The Perseus computational platform for comprehensive analysis of (prote)omics data. Nature Methods, 13(9), 731-740. https://doi.org/10.1038/nmeth.3901

Van Wijk, K. J. (2024). Intra-chloroplast proteases: A holistic network view of chloroplast proteolysis. The Plant Cell, 36(9), 3116-3130. https://doi.org/10.1093/plcell/koae178

Wang, Y., Wang, Y., Zhu, X., Ren, Y., Dong, H., Duan, E., Teng, X., Zhao, H., Chen, R., Chen, X., Lei, J., Yang, H., Tian, Y., Chen, L., Liu, X., Liu, S., Jiang, L., Wang, H., & Wan, J. (2023). Tetrapyrrole biosynthesis pathway regulates plastid-to-nucleus signaling by controlling plastid gene expression in plants. Plant Communications, 4(1), 100411. https://doi.org/10.1016/j.xplc.2022.100411

Wu, G.-Z., & Bock, R. (2021). GUN control in retrograde signaling: How GENOMES UNCOUPLED proteins adjust nuclear gene expression to plastid biogenesis. The Plant Cell, 33(3), 457-474. https://doi.org/10.1093/plcell/koaa048

Wu, G.-Z., Chalvin, C., Hoelscher, M., Meyer, E. H., Wu, X. N., & Bock, R. (2018). Control of Retrograde Signaling by Rapid Turnover of GENOMES UNCOUPLED1. Plant Physiology, 176(3), 2472-2495. https://doi.org/10.1104/pp.18.00009

Wu, G.-Z., Meyer, E. H., Richter, A. S., Schuster, M., Ling, Q., Schöttler, M. A., Walther, D., Zoschke, R., Grimm, B., Jarvis, R. P., & Bock, R. (2019). Control of retrograde signalling by protein import and cytosolic folding stress. Nature Plants, 5(5), 525-538. https://doi.org/10.1038/s41477-019-0415-y

Wu, G.-Z., Meyer, E. H., Wu, S., & Bock, R. (2019). Extensive Posttranscriptional Regulation of Nuclear Gene Expression by Plastid Retrograde Signals. Plant Physiology, 180(4), 2034-2048. https://doi.org/10.1104/pp.19.00421

Yoneda, T., Benedetti, C., Urano, F., Clark, S. G., Harding, H. P., & Ron, D. (2004). Compartment-specific perturbation of protein handling activates genes encoding mitochondrial chaperones. Journal of Cell Science, 117(18), 4055-4066. https://doi.org/10.1242/jcs.01275

Yoshioka-Nishimura, M., & Yamamoto, Y. (2014). Quality control of Photosystem II: The molecular basis for the action of FtsH protease and the dynamics of the thylakoid membranes. Journal of Photochemistry and Photobiology B: Biology, 137, 100-106. https://doi.org/10.1016/j.jphotobiol.2014.02.012

Zhao, Q., Wang, J., Levichkin, I. V., Stasinopoulos, S., Ryan, M. T., & Hoogenraad, N. J. (2002). A mitochondrial specific stress response in mammalian cells. The EMBO Journal, 21(17), 4411-4419. https://doi.org/10.1093/emboj/cdf445

Zhao, X., Huang, J., & Chory, J. (2018). Genome uncoupled1 Mutants Are Hypersensitive to Norflurazon and Lincomycin. Plant Physiology, 178(3), 960-964. https://doi.org/10.1104/pp.18.00772